

UNCLASSIFIED



# RESEARCH MEMORANDUM

STATIC LONGITUDINAL AND LATERAL STABILITY DATA FROM AN  
EXPLORATORY INVESTIGATION AT MACH NUMBER 4.06 OF AN  
AIRPLANE CONFIGURATION HAVING A WING  
OF TRAPEZOIDAL PLAN FORM

By Robert W. Dunning and Edward F. Ulmann

Langley Aeronautical Laboratory  
Langley Field, Va.

CLASSIFIED DOCUMENT

This material contains information affecting the National Defense of the United States within the meaning of the espionage laws, Title 18, U.S.C., Secs. 793 and 794, the transmission or revelation of which in any manner to an unauthorized person is prohibited by law.

**NATIONAL ADVISORY COMMITTEE  
FOR AERONAUTICS**

**WASHINGTON**

February 15, 1955

~~CONFIDENTIAL~~

## NATIONAL ADVISORY COMMITTEE FOR AERONAUTICS

## RESEARCH MEMORANDUM

STATIC LONGITUDINAL AND LATERAL STABILITY DATA FROM AN  
EXPLORATORY INVESTIGATION AT MACH NUMBER 4.06 OF AN  
AIRPLANE CONFIGURATION HAVING A WING  
OF TRAPEZOIDAL PLAN FORM

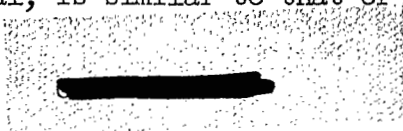
By Robert W. Dunning and Edward F. Ulmann

## SUMMARY

An investigation to determine the static longitudinal and lateral stability characteristics of an airplane configuration having a trapezoidal wing with modified hexagonal airfoil section and a cruciform tail with  $5^\circ$  semiangle wedge section has been carried out in the Langley 9- by 9-inch Mach number 4 blowdown jet. Tests on the complete airplane and various combinations of its components were made at a Mach number of 4.06 and a Reynolds number of  $2.7 \times 10^6$ , based on wing mean aerodynamic chord. Data were obtained for angles of attack from  $0^\circ$  to a maximum of  $8^\circ$  to  $20^\circ$ , at angles of sideslip from  $0^\circ$  up to a maximum of  $5^\circ$  to  $8^\circ$ , the maximum values depending on the configuration tested. The data are presented with respect to body axes except for lift and drag which are referred to the stability axes.

## INTRODUCTION

The aircraft configurations previously investigated experimentally at high supersonic and hypersonic speeds have been restricted to missiles which were not required to land, and which therefore had relatively small wings or wings of very low aspect ratio. The purpose of the present investigation was to determine the characteristics of a configuration conforming more closely to a piloted aircraft having a wing area sufficient for conventional landing. Of the various possible configurations, one was selected for this exploratory study which was expected to have satisfactory low-speed characteristics and satisfactory transonic characteristics. This configuration (fig. 1) employs a trapezoidal wing and the arrangement, in general, is similar to that of conventional airplanes.



Two particular features were incorporated which are believed to be desirable for high supersonic and hypersonic operation - relatively large leading-edge radii for both wing and tail and wedge-shaped sections for the tail surfaces. The wing and tail sections were designed with large leading-edge radii because of heat-transfer considerations at high Mach numbers. The wing leading-edge radius, for example, would be approximately 1.5 inches at the wing-fuselage intersection for a full-size airplane having a wing span of about 28 feet. Inasmuch as the effectiveness of lifting surfaces having flat-plate or conventional airfoil sections decreases considerably with Mach number at high supersonic speeds (ref. 1), the effectiveness of tail surfaces of conventional size utilizing these airfoil sections would be marginal or insufficient at the Mach number of the present tests. Several types of tail airfoil sections therefore are being considered and the present results were obtained with a  $5^\circ$  semiangle wedge section.

In references 2 and 3, longitudinal and lateral stability data were presented for this same configuration at Mach number 6.86. This report presents the static longitudinal and lateral stability characteristics at Mach number 4.06 without analysis in order to expedite publication.

#### SYMBOLS

The results of the tests are presented as standard NACA coefficients of forces and moments. The data are referred to the body axes except for lift and drag which are referred to the stability axes (fig. 2), with the reference center of gravity at 52.66 percent body length from the body nose (54 percent mean aerodynamic chord).

$C_N$	normal-force coefficient, $-Z_B/qS$
$C_L$	lift coefficient, $-Z_S/qS$
$C_{D_T}$	total drag coefficient, $-X_{B_T}/qS$
$C_{D_B}$	base drag coefficient, $-X_{B_B}/qS$
$C_{m_{c.g.}}$	pitching-moment coefficient about center of gravity, $M'/qS\bar{c}$
$C_Y$	lateral-force coefficient, $Y/qS$
$C_n$	yawing-moment coefficient about center of gravity, $N/qSb$

$C_L$	rolling-moment coefficient, $L/qSb$
$Z_B$	force along $Z_B$ -axis
$Z_S$	force along $Z_S$ -axis
$X_{BT}$	total force along $X_B$ -axis
$X_{BB}$	force along $X_B$ -axis contributed by base
$M'$	moment about Y-axis
$Y$	force along Y-axis
$N$	moment about $Z_B$ -axis
$L$	moment about $X_B$ -axis
$q$	free-stream dynamic pressure
$S$	total wing area, including body intercept
$\bar{c}$	wing mean aerodynamic chord
$b$	wing span
$L/D_T$	lift-drag ratio, $C_L/C_{D_T}$
$R$	Reynolds number based on $\bar{c}$
$M$	Mach number
c.p.	longitudinal distance from nose to center of pressure, percent body length
$\alpha$	angle of attack of fuselage center line, deg
$\beta$	angle of sideslip, deg
$\frac{\partial C_m}{\partial C_L}$	rate of change of pitching-moment coefficient with lift coefficient
$C_{n_\beta}$	rate of change of yawing-moment coefficient with angle of sideslip

$C_{l\beta}$	rate of change of rolling-moment coefficient with angle of sideslip
$C_{Y\beta}$	rate of change of lateral-force coefficient with angle of sideslip

### APPARATUS

The tests were conducted in the Langley 9- by 9-inch Mach number 4 blowdown jet, which is described and for which a calibration is given in reference 4. The settling-chamber pressure, which was held constant by a pressure-regulating valve, and the corresponding air temperature were continuously recorded during each run.

Two separate internal strain-gage balances were used to obtain the data. One balance measured normal force, pitching moment, side force, yawing moment, and rolling moment. The second balance measured chord force through the angle-of-attack range but was limited to measurements at zero angle of sideslip because of balance design.

Representative schlieren photographs of the flow around the model were made by the use of an off-axis, single-pass, two-mirror schlieren system. Exposure time was 1/200 second, and the knife edge was oriented parallel to the free-stream flow.

### MODELS

The model configurations used for the present tests consisted of a complete airplane (fig. 1), a body alone, a body-wing combination, and a body-tail combination. Details concerning the airplane model are given in the three-view drawing (fig. 3(a)), in the sketches of the airfoil sections (fig. 3(b)), and in the table of geometric characteristics (table I). The wing and tail sections were designed with large leading-edge radii because of heat-transfer considerations at high Mach numbers. A photograph of the complete airplane configuration installed in the Langley 9- by 9-inch Mach number 4 blowdown jet is presented in figure 4.

### TESTS

The settling-chamber stagnation temperature during any single run varied from approximately 80° to 40° F, and the settling-chamber stagnation pressure was held at approximately 186 lb/sq in. abs. These conditions correspond approximately to a Reynolds number of  $2.7 \times 10^6$ , based

on the wing mean aerodynamic chord. The tests were run at humidities below  $5 \times 10^{-6}$  pounds of water vapor per pound of dry air, which is believed to be low enough to eliminate water-condensation effects. The test-section static temperature and pressure did not reach the point where liquefaction of air would take place. Data were obtained for angles of attack from  $0^\circ$  to a maximum of  $8^\circ$  to  $20^\circ$ , at angles of sideslip from  $0^\circ$  to a maximum of  $5^\circ$  to  $8^\circ$ , the maximum values depending on the configuration tested. Base drag data were obtained from static pressures measured at the base of the model.

### PRECISION OF DATA

The probable uncertainties in the test data due to the accuracy limitations of the balances and the recording equipment and the ability of the system to repeat data points are listed in the table below. The low accuracy of the rolling-moment coefficients relative to the maximum rolling-moment encountered should be noted. This occurred because rolling-moment gages were added to an existing balance which was not originally designed to measure rolling moment.

$C_N$	±0.001
$C_L$	±0.001
$C_{D_T}$	±0.0003
$C_{m.c.g.}$	±0.0004
$C_Y$	±0.0003
$C_n$	±0.00005
$C_l$	±0.0009
$\alpha$ , deg	±0.1
$\beta$ , deg	±0.1

### RESULTS

The experimental static aerodynamic characteristics of the models are given for all angles of attack and sideslip in tables II and III, and representative portions of the data are presented in the figures. Equations for transferring these coefficients from the body axes to the stability axes are presented in the appendix. The variations with angle of attack of the longitudinal characteristics of the complete airplane and various combinations of its components are presented in figures 5

to 11. In figures 12 and 13 some static longitudinal stability characteristics are presented.

The variations with sideslip angle of the lateral characteristics of the body-wing and complete-airplane configurations are presented in figure 14, and the variations with sideslip angle of the longitudinal characteristics of the body-wing and complete-airplane configurations are presented in figure 15. The effects of normal-force coefficient on the lateral characteristics for the body-wing and complete configurations are presented in figure 16. Some static lateral stability characteristics are presented in figure 17.

Typical schlieren photographs of the components at a constant angle of attack and of the complete model at various angles of attack are presented in figures 18 and 19. The closely spaced disturbances which can be seen extending downstream at the top and the bottom of the schlieren field of view are caused by the tips of 1/4-inch-diameter rods which support the model against shock loads during the starting and stopping cycles of the tunnel. The rods are withdrawn into or almost into the tunnel floor and ceiling while data are being taken. The plugged holes in the tunnel floor used for these rods may be seen in figure 4. It should be noted that the model pivots in pitch about a point near the base of the body, and that consequently the tail fins do not move up or down into that part of the flow influenced by the disturbances from the support rods.

Langley Aeronautical Laboratory,  
National Advisory Committee for Aeronautics,  
Langley Field, Va., January 3, 1955.

## APPENDIX

The equations for transfer of force and moment coefficients from the body-axis system to the stability-axis system (fig. 2) are as follows:

$$C_{Y_S} = C_{Y_B}$$

$$C_{l_S} = C_{l_B} \cos \alpha + C_{n_B} \sin \alpha$$

$$C_{n_S} = C_{n_B} \cos \alpha - C_{l_B} \sin \alpha$$

$$C_{m_S} = C_{m_B}$$

Since longitudinal forces were measured only for  $\beta = 0$ , the axis-transfer equations for  $C_{L_S}$  and  $C_{D_S}$  are not given here.



## REFERENCES

1. McLellan, Charles H.: A Method for Increasing the Effectiveness of Stabilizing Surfaces at High Supersonic Mach Numbers. NACA RM L54F21, 1954.
2. Penland, Jim A., Ridyard, Herbert W., and Fetterman, David E., Jr.: Lift, Drag, and Static Longitudinal Stability Data From an Exploratory Investigation at a Mach Number of 6.86 of an Airplane Configuration Having a Wing of Trapezoidal Plan Form. NACA RM L54L03b, 1955.
3. Ridyard, Herbert W., Fetterman, David E., Jr., and Penland, Jim A.: Static Lateral Stability Data From an Exploratory Investigation at a Mach Number of 6.86 of an Airplane Configuration Having a Wing of Trapezoidal Plan Form. NACA RM L55A21a, 1955.
4. Ulmann, Edward F., and Lord, Douglas R.: An Investigation of Flow Characteristics at Mach Number 4.04 Over 6- and 9-Percent-Thick Symmetrical Circular-Arc Airfoils Having 30-Percent-Chord Trailing-Edge Flaps. NACA RM L51D30, 1951.

TABLE I.- GEOMETRIC CHARACTERISTICS OF MODEL

## Wing:

Area (including area submerged in fuselage), sq in. . . . .	6.24
Span, in. . . . .	4.33
Mean aerodynamic chord, in. . . . .	1.716
Root chord, in. . . . .	2.53
Tip chord, in. . . . .	0.354
Airfoil section . . . . .	hexagonal with round leading edge
Taper ratio . . . . .	0.140
Aspect ratio . . . . .	3.00
Sweep of leading edge, deg . . . . .	38.83
Sweep of quarter-chord line, deg . . . . .	29
Incidence at fuselage center line, deg . . . . .	0
Dihedral, deg . . . . .	0
Geometric twist, deg . . . . .	0

## Horizontal tail or vertical tail:

Area (including area submerged in fuselage), sq in. . . . .	2.06
Span, in. . . . .	2.69
Mean aerodynamic chord, in. . . . .	0.853
Root chord, in. . . . .	1.214
Tip chord, in. . . . .	0.317
Airfoil section . . . . .	5° semiangle wedge
Taper ratio . . . . .	0.261
Aspect ratio . . . . .	3.52
Sweep of leading edge, deg . . . . .	22.63
Dihedral, deg . . . . .	0

## Fuselage:

Length, in. . . . .	7.50
Maximum diameter, in. . . . .	0.790
Fineness ratio . . . . .	9.50
Base diameter, in. . . . .	0.790
Distance from nose to moment reference . . . . .	3.950
Ogive nose length, in. . . . .	2.29
Ogive radius, in. . . . .	6.85

TABLE II.- STATIC LONGITUDINAL AND LATERAL AERODYNAMIC CHARACTERISTICS  
OF AN AIRPLANE CONFIGURATION AND VARIOUS COMBINATIONS OF ITS  
COMPONENTS. BODY AXIS DATA.  $M = 4.06$ .  $R = 2.7 \times 10^6$ .

## (a) Body-wing-tail

$\alpha$	$\beta$	$C_N$	$C_{m.c.g.}$	c.p.	$C_Y$	$C_n$	$C_l$
0.0 ↓	0.0	-0.0023	0.0001	53.7	-0.0001	0.0001	0.0009
	1.0	-.0023	.0002	54.7	-.0110	.0026	.0008
	2.0	-.0017	0.0	52.7	-.0223	.0050	.0007
	3.0	-.0017	0.0	52.7	-.0341	.0077	.0004
	4.0	-.0016	0.0	52.7	-.0454	.0102	.0003
	5.0	-.0048	.0011	57.9	-.0570	.0124	.0004
2.0 ↓	0.0	0.0484	-0.0125	58.6	0.0010	0.0	.0002
	1.0	.0484	-.0127	58.7	-.0102	.0025	.0001
	2.0	.0483	-.0129	58.8	-.0215	.0050	0.0
	3.0	.0472	-.0129	58.9	-.0334	.0076	0.0
	4.0	.0466	-.0131	59.1	-.0451	.0101	.0006
	5.0	.0461	-.0131	59.2	-.0571	.0124	.0006
4.0 ↓	0.0	0.1002	-0.0248	58.3	0.0020	-0.0002	0.0
	0.0	.1009	-.0253	58.4	.0019	-.0002	.0011
	0.0	.1019	-.0256	58.4	.0024	-.0002	-.0004
	1.0	.1025	-.0255	58.4	-.0098	.0023	.0014
	1.0	.1020	-.0256	58.4	-.0095	.0023	-.0003
	2.0	.1025	-.0257	58.4	-.0208	.0048	.0015
	2.0	.1016	-.0257	58.5	-.0206	.0047	-.0002
	3.0	.1032	-.0256	58.4	-.0329	.0074	.0011
	3.0	.1019	-.0258	58.5	-.0330	.0074	0.0
	4.0	.1037	-.0256	58.3	-.0458	.0101	.0009
	4.0	.1019	-.0259	58.5	-.0455	.0100	.0002
	5.0	.1038	-.0258	58.4	-.0579	.0125	.0009
	5.0	.1024	-.0262	58.5	-.0575	.0125	0.0
	6.0	.1024	-.0262	58.5	-.0575	.0125	0.0
6.0 ↓	0.0	0.1614	-0.0408	58.5	0.0029	-0.0003	0.0001
	1.0	.1554	-.0387	58.4	-.0091	.0024	.0001
	2.0	.1546	-.0380	58.3	-.0204	.0047	.0004
	3.0	.1557	-.0378	58.2	-.0335	.0074	.0004
	4.0	.1554	-.0374	58.2	-.0450	.0099	.0006

TABLE II. - STATIC LONGITUDINAL AND LATERAL AERODYNAMIC CHARACTERISTICS OF AN  
AIRPLANE CONFIGURATION AND VARIOUS COMBINATIONS OF ITS COMPONENTS.

BODY AXIS DATA.  $M = 4.06$ .  $R = 2.7 \times 10^6$  - Continued

(a) Body-wing-tail - Concluded

$\alpha$	$\beta$	$C_N$	$C_{m_{c.g.}}$	c.p.	$C_Y$	$C_n$	$C_l$
8.0	0.0	0.2142	-0.0534	58.4	0.0033	-0.0003	-0.0004
↓	1.0	.2142	-.0531	58.3	-.0098	.0025	-.0002

(b) Body

0.0	0.0	-0.0017	-0.0011	37.9	-0.0002	0.0001	0.0005
2.0	0.0	.0067	.0085	23.6	.0001	.0002	.0009
4.0	0.0	.0178	.0184	29.0	.0003	.0003	.0009
6.0	0.0	.0327	.0248	35.3	.0005	.0002	.0008
8.0	0.0	.0502	.0271	40.3	.0011	.0002	.0007
10.0	0.0	.0709	.0301	43.0	.0011	.0002	.0004
12.0	0.0	.0908	.0338	44.2	.0017	.0003	.0001
14.0	0.0	.1119	.0378	44.9	.0022	.0004	-.0004
15.0	0.0	.1220	.0390	45.4	.0019	.0003	.0009
16.0	0.0	.1326	.0398	45.8	.0021	.0004	.0008
18.0	0.0	.1585	.0401	46.9	.0026	.0004	.0003
20.0	0.0	.1858	.0402	47.7	.0043	.0003	.0002

(c) Body-wing

0.0	0.0	0.0045	0.0009	48.1	0.0007	0.0001	0.0015
↓	1.0	.0050	.0009	48.6	-.0034	-.0016	.0013
	2.0	.0029	.0007	47.2	-.0083	-.0034	.0013
	3.0	.0025	.0005	48.1	-.0129	-.0051	.0010
	4.0	.0004	0.0	52.7	-.0182	-.0067	.0006
	5.0	-.0011	-.0003	46.4	-.0236	-.0080	.0003
	6.0	-.0021	-.0004	48.3	-.0307	-.0091	-.0001
	7.0	-.0006	-.0001	48.9	-.0387	-.0098	.0004
	8.0	-.0001	0.0	52.7	-.0477	-.0103	.0007

TABLE II.- STATIC LONGITUDINAL AND LATERAL AERODYNAMIC CHARACTERISTICS  
OF AN AIRPLANE CONFIGURATION AND VARIOUS COMBINATIONS OF ITS  
COMPONENTS. BODY AXIS DATA.  $M = 4.06$ .

$R = 2.7 \times 10^6$  - Continued

(c) Body-wing - Continued

$\alpha$	$\beta$	$C_N$	$C_{m.c.g.}$	c.p.	$C_Y$	$C_n$	$C_l$
2.0	0.0	0.0368	0.0041	50.1	0.0009	0.0002	0.0001
↓	1.0	.0372	.0044	50.0	-.0035	-.0016	.0001
	2.0	.0366	.0047	49.7	-.0078	-.0033	.0
	3.0	.0365	.0048	49.7	-.0130	-.0050	-.0001
	4.0	.0364	.0049	49.6	-.0180	-.0067	.0001
	5.0	.0375	.0051	49.6	-.0238	-.0080	.0001
	6.0	.0380	.0053	49.5	-.0308	-.0091	-.0002
	7.0	.0385	.0054	49.5	-.0389	-.0099	-.0003
↓	8.0	.0383	.0052	49.6	-.0473	-.0103	.0005
4.0	0.0	0.0812	0.0092	50.1	0.0019	0.0004	0.0010
↓	1.0	.0818	.0095	50.0	-.0028	-.0016	.0007
	2.0	.0825	.0100	49.9	-.0071	-.0032	.0007
	3.0	.0822	.0103	49.8	-.0123	-.0050	.0004
	4.0	.0824	.0107	49.7	-.0175	-.0065	.0003
	5.0	.0831	.0110	49.6	-.0237	-.0079	.0003
	6.0	.0837	.0110	49.7	-.0308	-.0090	.0002
	7.0	.0847	.0110	49.7	-.0394	-.0100	.0
↓	8.0	.0855	.0108	49.8	-.0472	-.0105	.0001
6.0	0.0	0.1262	0.0137	50.2	0.0021	0.0003	0.0008
↓	1.0	.1259	.0138	50.2	-.0027	-.0017	.0007
	2.0	.1259	.0141	50.1	-.0073	-.0035	.0006
	3.0	.1266	.0149	50.0	-.0132	-.0054	.0005
	4.0	.1266	.0153	49.9	-.0186	-.0068	.0005
	5.0	.1273	.0154	49.9	-.0248	-.0082	.0004
	6.0	.1289	.0156	49.9	-.0321	-.0094	.0003
	7.0	.1296	.0158	49.9	-.0407	-.0104	.0001
↓	8.0	.1302	.0159	49.9	-.0486	-.0109	-.0002
6.1							
8.0	0.0	0.1730	0.0165	50.5	0.0026	0.0003	.0007
↓	1.0	.1727	.0167	50.5	-.0027	-.0016	.0008
	2.0	.1727	.0170	50.4	-.0080	-.0035	.0005
	3.0	.1722	.0176	50.3	-.0138	-.0053	.0003
	4.0	.1728	.0184	50.2	-.0200	-.0068	.0
	5.0	.1735	.0191	50.2	-.0266	-.0082	-.0001
	5.9	.1746	.0200	50.1	-.0335	-.0096	-.0009
↓	8.1	.1760	.0204	50.0	-.0420	-.0104	-.0008
8.1	7.9	.1775	.0208	50.0	-.0506	-.0110	-.0009

TABLE II.- STATIC LONGITUDINAL AND LATERAL AERODYNAMIC CHARACTERISTICS  
OF AN AIRPLANE CONFIGURATION AND VARIOUS COMBINATIONS OF ITS  
COMPONENTS. BODY AXIS DATA.  $M = 4.06$ .

$R = 2.7 \times 10^6$  - Continued

(c) Body-wing - Concluded

$\alpha$	$\beta$	$C_N$	$C_{m.c.g.}$	c.p.	$C_Y$	$C_n$	$C_l$
10.0 ↓	0.0	0.2275	0.0185	50.8	0.0038	0.0003	-0.0001
	1.0	.2278	.0189	50.8	-.0027	-.0015	-.0005
	2.0	.2279	.0195	50.7	-.0086	-.0032	-.0006
	3.0	.2279	.0200	50.7	-.0154	-.0051	-.0008
	3.9	.2274	.0213	50.5	-.0220	-.0065	-.0012
	4.9	.2234	.0225	50.4	-.0292	-.0077	-.0013
10.1	5.9	.2251	.0234	50.3	-.0366	-.0089	-.0014
10.1	6.9	.2267	.0243	50.2	-.0449	-.0100	-.0015
10.1	7.9	.2271	.0250	50.2	-.0538	-.0110	-.0017
12.0 ↓	0.0	0.2858	0.0196	51.1	0.0040	0.0004	-0.0004
	1.0	.2855	.0194	51.1	-.0030	-.0013	-.0009
	2.0	.2850	.0199	51.1	-.0097	-.0028	-.0011
	2.9	.2851	.0211	51.0	-.0176	-.0045	-.0013
	3.9	.2834	.0232	50.8	-.0244	-.0057	-.0023
	4.9	.2811	.0247	50.7	-.0324	-.0068	-.0027
12.1	5.9	.2819	.0262	50.5	-.0408	-.0079	-.0028
12.1	6.9	.2818	.0278	50.4	-.0494	-.0090	-.0032
12.1	7.8	.2824	.0292	50.3	-.0577	-.0100	-.0031

(d) Body-tail

0.0 ↓	0.0	-0.0027	0.0002	54.4	-0.0006	0.0	0.0002
	1.0	-.0027	.0002	54.4	-.0119	.0025	.0001
	2.0	-.0033	.0	52.7	-.0232	.0050	.0006
	3.0	-.0038	.0003	54.5	-.0355	.0077	.0007
	4.0	-.0033	.0004	55.4	-.0469	.0102	.0008
	5.0	-.0027	.0004	56.1	-.0586	.0128	.0005
2.0 ↓	0.0	0.0202	-0.0113	65.5	0.0001	-0.0001	0.0004
	1.0	.0202	-.0113	65.5	-.0114	.0026	.0003
	2.0	.0202	-.0116	65.8	-.0225	.0051	.0002
	3.0	.0202	-.0118	66.0	-.0348	.0078	.0
	4.0	.0202	-.0119	66.2	-.0470	.0104	.0001
	5.0	.0206	-.0122	66.2	-.0586	.0128	.0005

TABLE II.- STATIC LONGITUDINAL AND LATERAL AERODYNAMIC CHARACTERISTICS  
OF AN AIRPLANE CONFIGURATION AND VARIOUS COMBINATIONS OF ITS  
COMPONENTS. BODY AXIS DATA.  $M = 4.06$ .

$R = 2.7 \times 10^6$  - Concluded

(d) Body-tail - Concluded

$\alpha$	$\beta$	$C_N$	$C_{m_{c.g.}}$	c.p.	$C_Y$	$C_n$	$C_l$
4.0 ↓	0.0	0.0417	-0.0253	66.6	0.0008	-0.0001	-0.0003
	0.0	.0433	-.0246	65.7	.0013	-.0002	.0001
	1.0	.0422	-.0254	66.4	-.0114	.0025	.0002
	1.0	.0431	-.0246	65.7	-.0109	.0025	-.0001
	2.0	.0422	-.0255	66.5	-.0224	.0050	.0007
	2.0	.0431	-.0249	65.9	-.0221	.0050	-.0002
	3.0	.0427	-.0257	66.4	-.0347	.0077	.0006
	3.0	.0441	-.0254	65.9	-.0346	.0077	-.0001
	4.0	.0433	-.0260	66.4	-.0476	.0104	.0004
	4.0	.0445	-.0259	66.0	-.0474	.0104	.0005
	5.0	.0445	-.0264	66.2	-.0600	.0129	.0001
	5.0	.0445	-.0264	66.2	-.0599	.0129	.0007
6.0 ↓	0.0	0.0686	-0.0394	65.8	0.0015	-0.0002	0.0004
	1.0	.0691	-.0395	65.8	-.0110	.0026	.0003
	2.0	.0691	-.0397	65.8	-.0224	.0050	-.0001
	3.0	.0691	-.0393	65.7	-.0361	.0079	-.0003
	4.0	.0690	-.0396	65.8	-.0480	.0105	-.0003
8.0 ↓	0.0	0.0951	-0.0552	66.0	0.0016	-0.0002	0.0009
	1.0	.0953	-.0552	65.9	-.0113	.0025	.0007
	2.0	.0953	-.0547	65.8	-.0228	.0049	.0006

TABLE III.- STATIC LONGITUDINAL AERODYNAMIC CHARACTERISTICS OF AN  
AIRPLANE CONFIGURATION AND VARIOUS COMBINATIONS OF ITS  
COMPONENTS. STABILITY AXIS DATA.

$$M = 4.06. \quad R = 2.7 \times 10^6.$$

(a) Body-wing-tail

$\alpha$	$\beta$	$C_L$	$C_{D_T}$	$C_{D_B}$	$L/D_T$	$\alpha$	$\beta$	$C_L$	$C_{D_T}$	$C_{D_B}$	$L/D_T$
0.0	0.0	-0.0023	0.0439	0.0056	-0.05	6.0	0.0	0.1555	0.0646	0.0056	2.41
2.0	0.0	.0468	.0475	.0056	.99	8.0	0.0	.2053	.0780	.0055	2.63
4.0	0.0	.0975	.0534	.0056	1.83						
4.0	0.0	.0977	.0528	.0056	1.85						

(b) Body

0.0	0.0	-0.0017	0.0156	0.0053	-0.11	12.0	0.0	0.0847	0.0382	0.0058	2.22
2.0	0.0	.0061	.0165	.0053	.37	14.0	0.0	.1038	.0463	.0058	2.24
4.0	0.0	.0166	.0181	.0053	.92	15.0	0.0	.1127	.0509	.0058	2.21
6.0	0.0	.0307	.0209	.0053	1.47	16.0	0.0	.1219	.0558	.0058	2.18
8.0	0.0	.0471	.0256	.0058	1.84	18.0	0.0	.1446	.0680	.0058	2.13
10.0	0.0	.0665	.0312	.0058	2.13	20.0	0.0	.1676	.0829	.0058	2.02

(c) Body-wing

0.0	0.0	0.0045	0.0293	0.0052	0.15	8.0	0.0	0.1667	0.0567	0.0055	2.94
2.0	0.0	.0357	.0314	.0052	1.14	10.0	0.0	.2180	.0738	.0058	2.95
4.0	0.0	.0788	.0364	.0052	2.16	12.0	0.0	.2721	.0946	.0057	2.88
6.0	0.0	.1222	.0449	.0052	2.72						

(d) Body-tail

0.0	0.0	-0.0027	0.0329	0.0056	-0.08	6.0	0.0	0.0646	0.0414	0.0056	1.56
2.0	0.0	.0190	.0343	.0056	.55	8.0	0.0	.0892	.0484	.0055	1.84
4.0	0.0	.0408	.0367	.0056	1.11						
4.0	0.0	.0393	.0364	.0056	1.08						



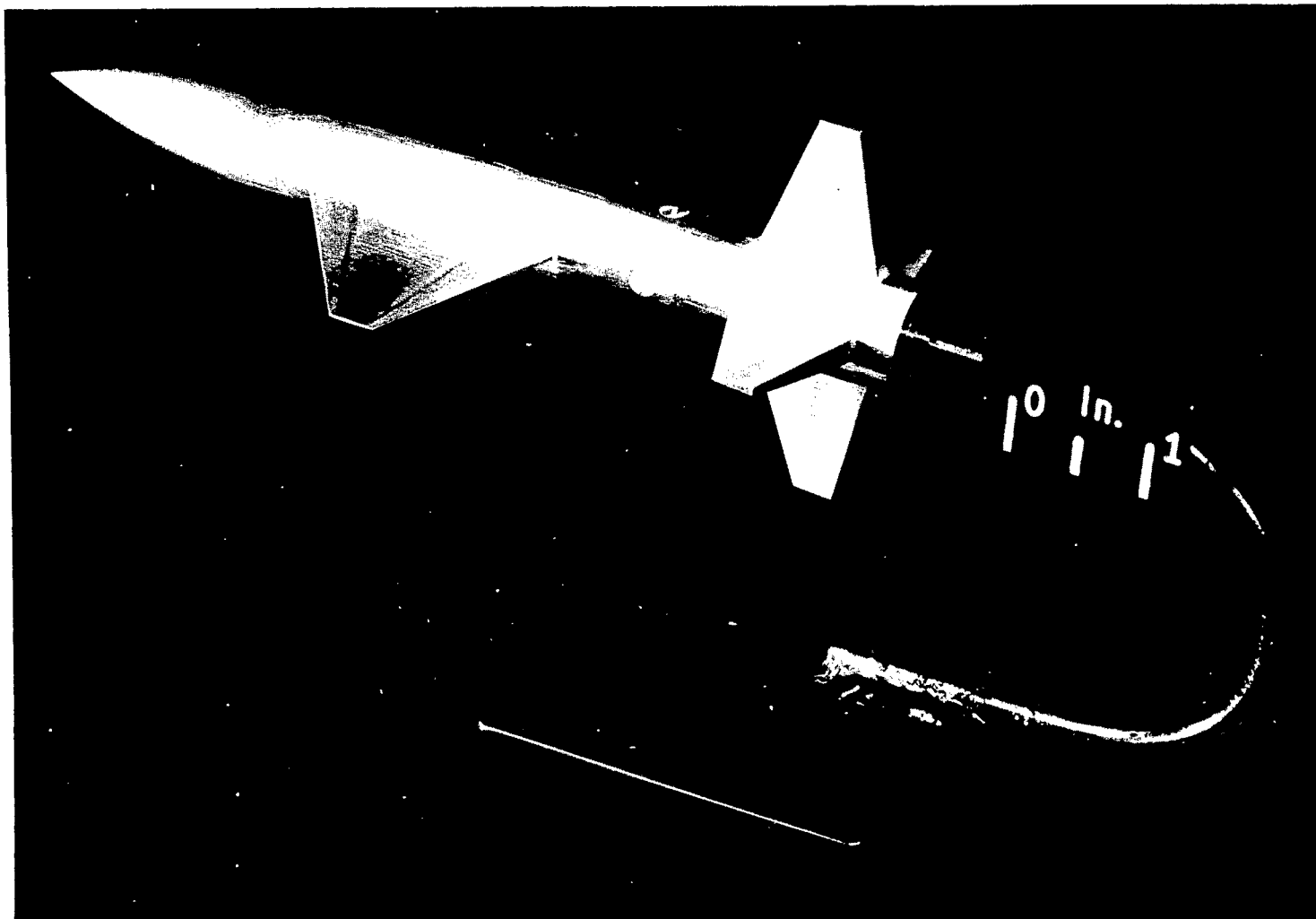


Figure 1.- Photograph of complete-model configuration. L-86688

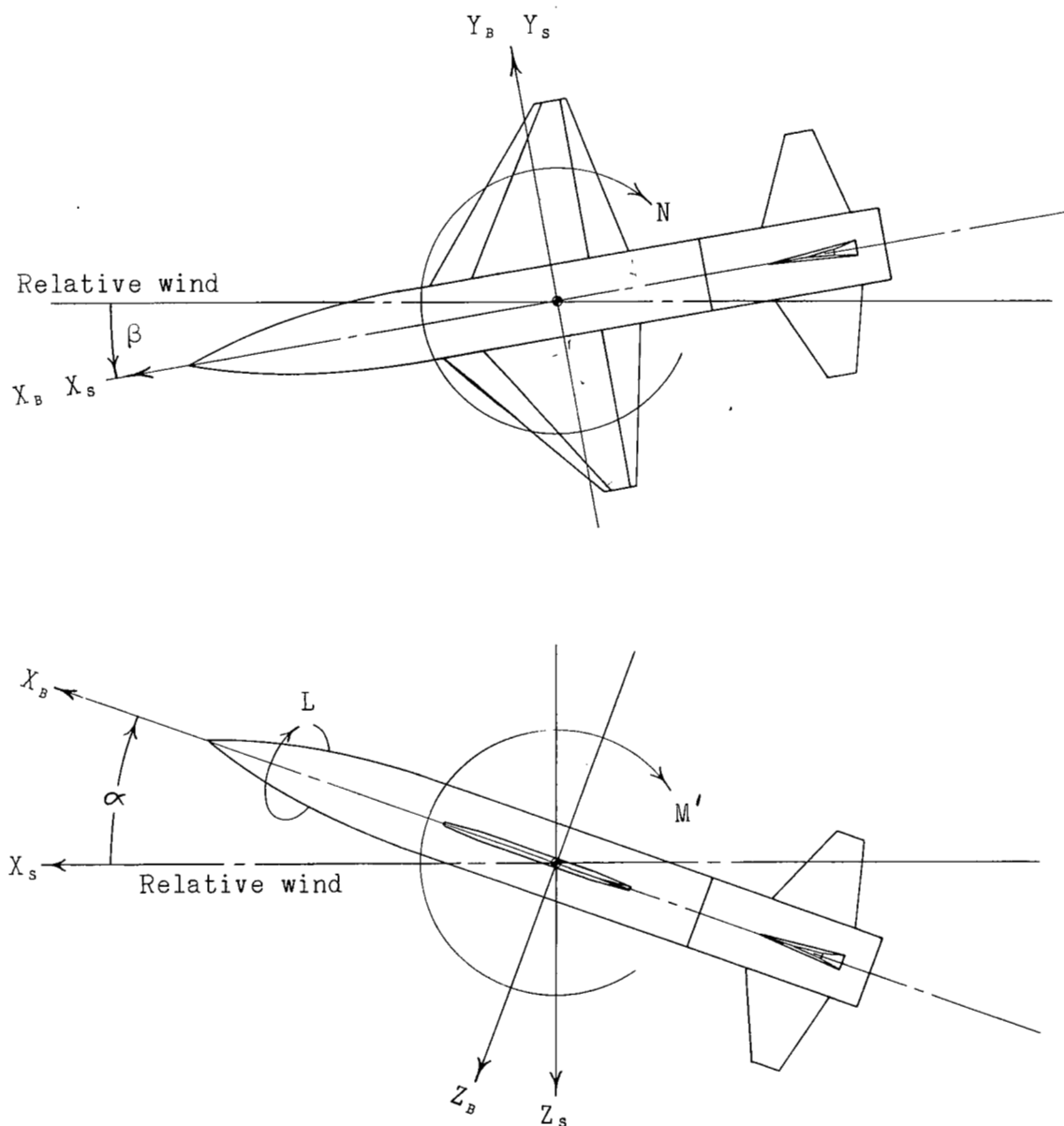


Figure 2.- Systems of reference axes. Subscript B indicates body axes; subscript S indicates stability axes.

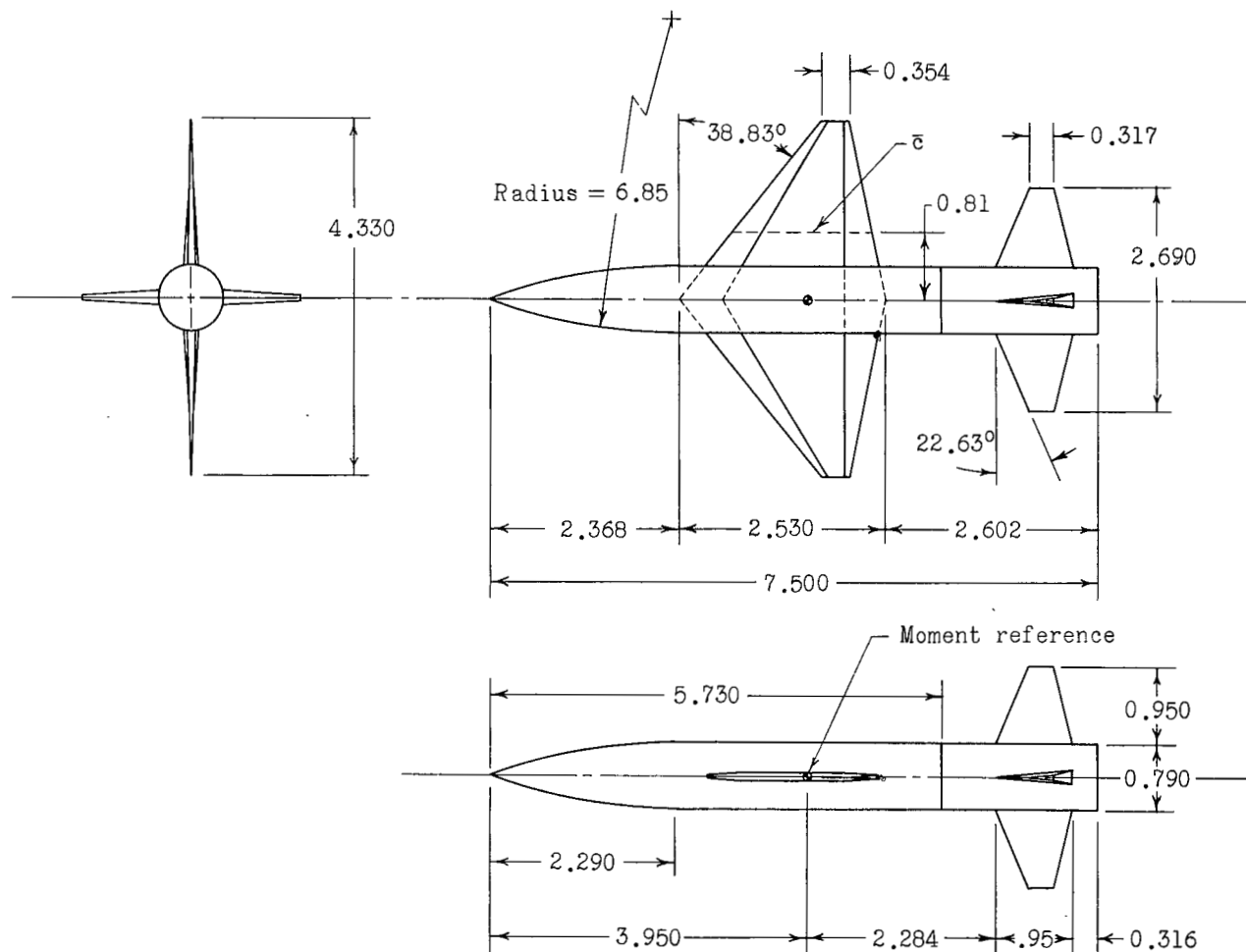
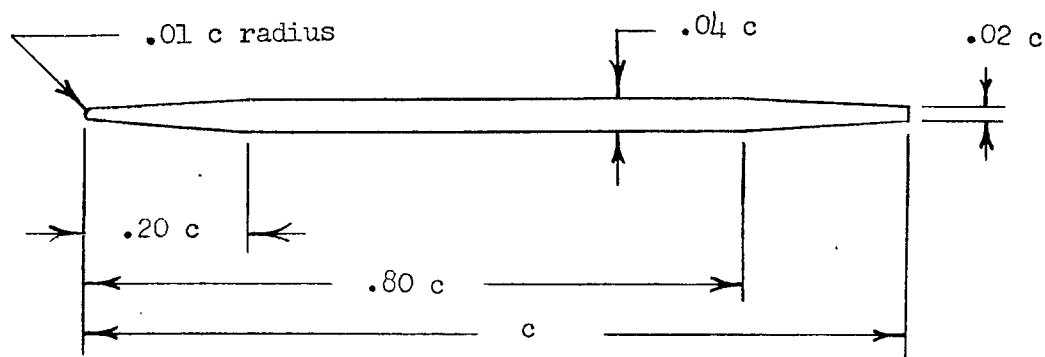
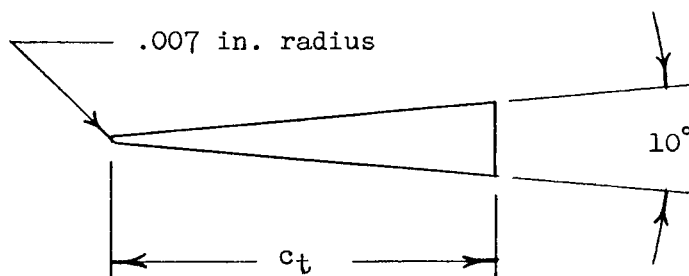


Figure 3(a).- Wind-tunnel model. All dimensions are in inches.

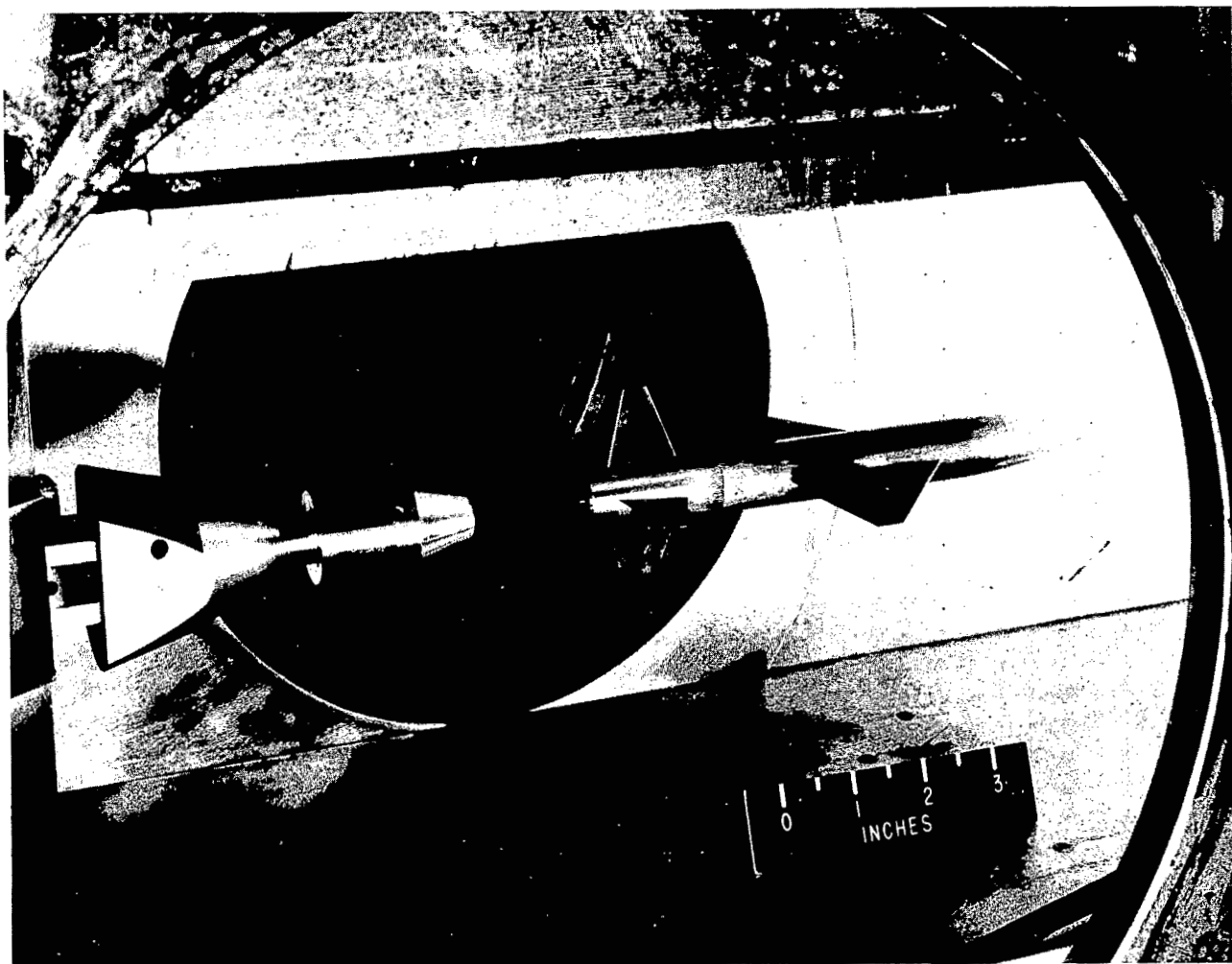


(a) Wing.

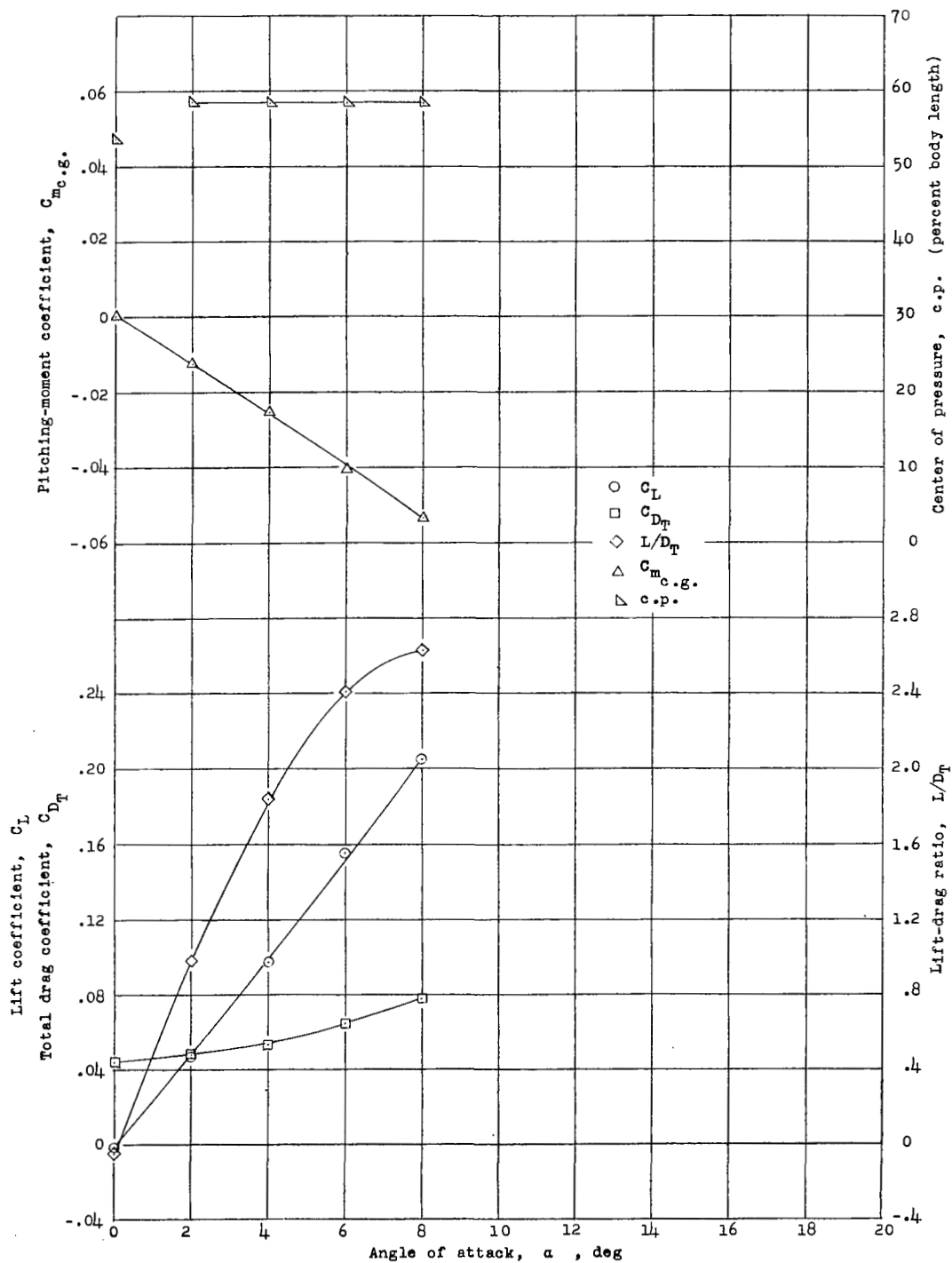


(b) Horizontal and vertical tails.

Figure 3(b).- Wing and tail airfoil sections used on model.

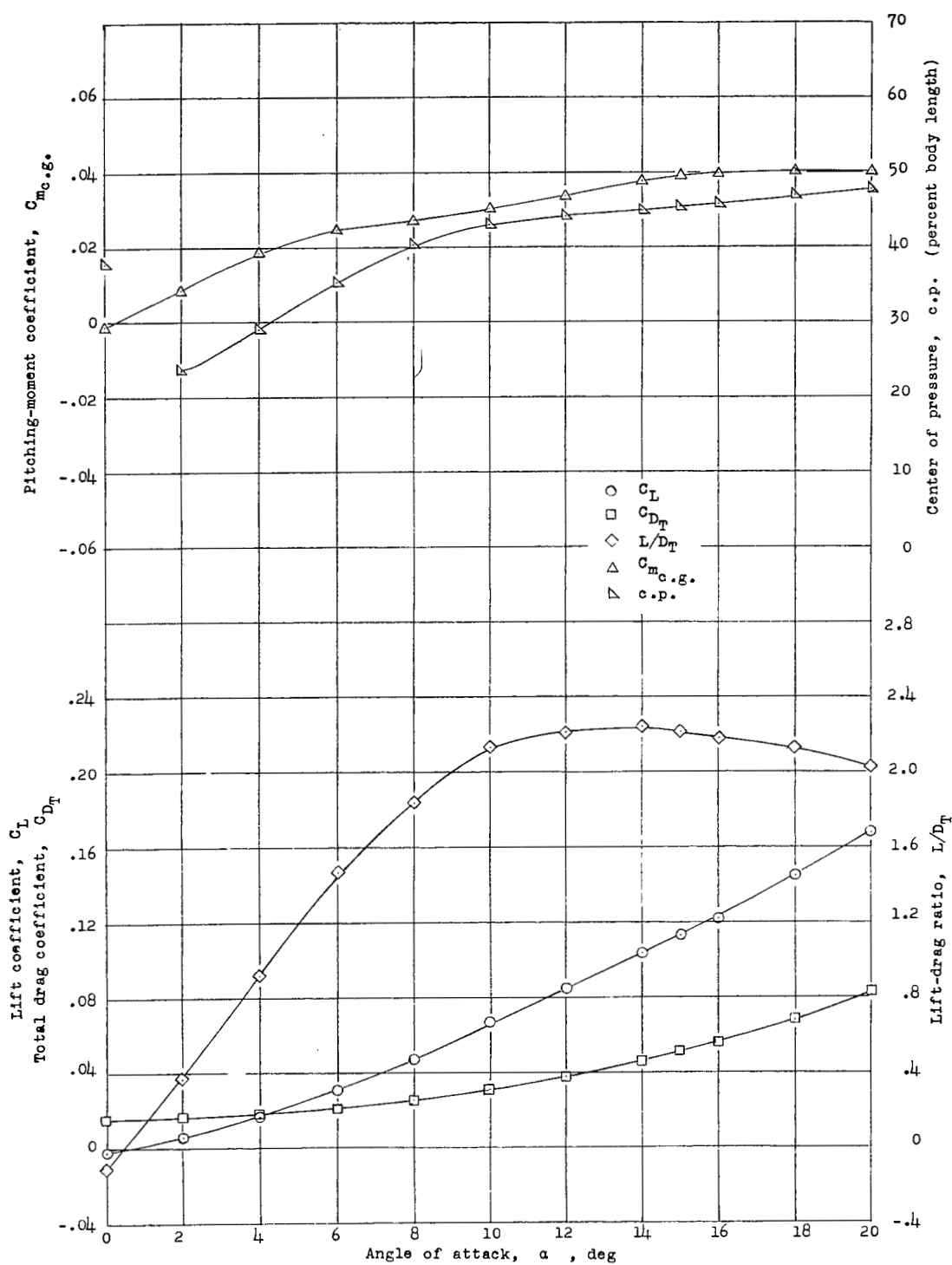


L-87425  
Figure 4.- Installation of the wind-tunnel model in the Langley 9- by  
9-inch Mach number 4 blowdown jet.



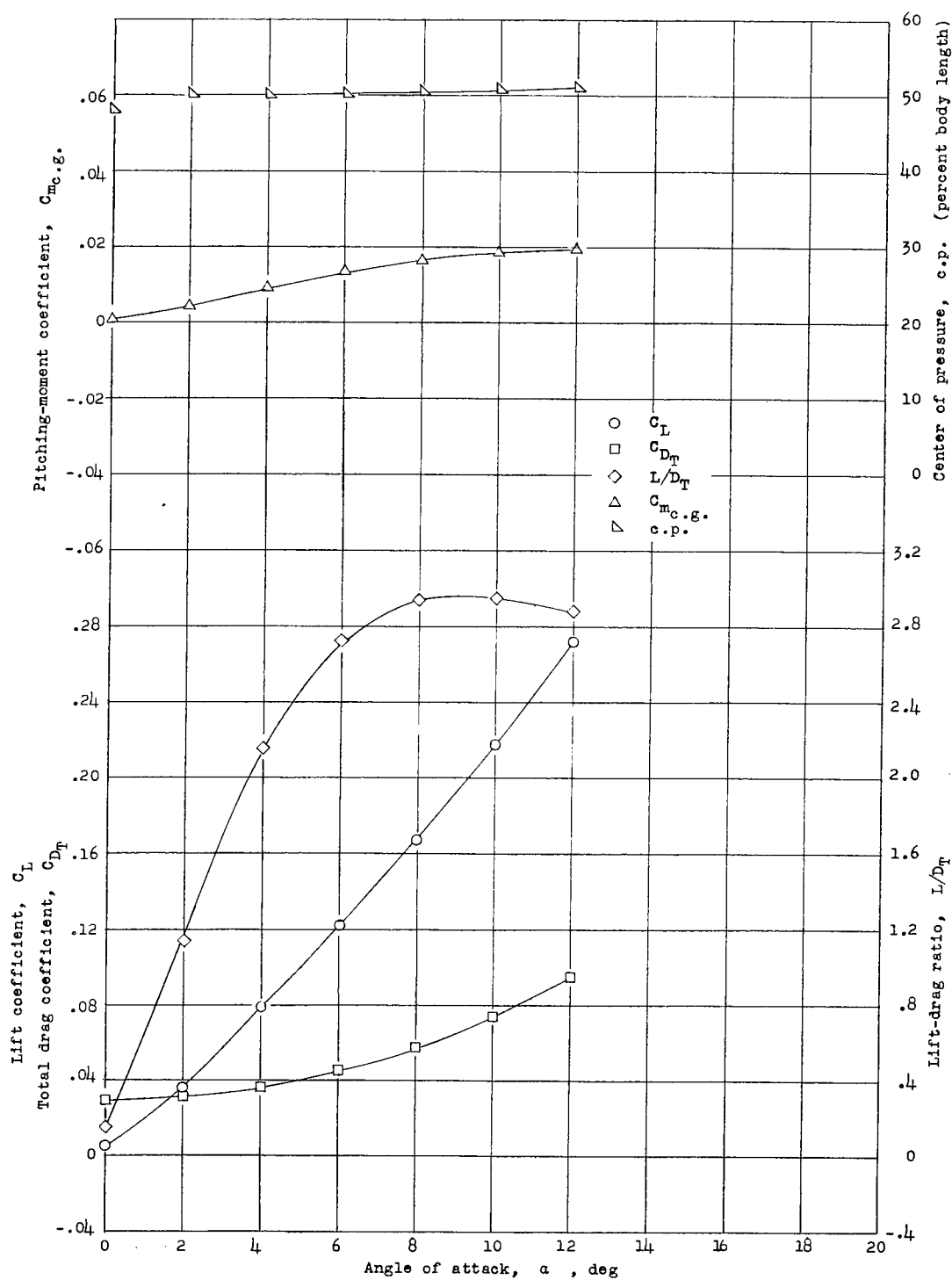
(a) Body-wing-tail.

Figure 5.- Variation with angle of attack of the static longitudinal characteristics of an airplane configuration and its components.  
 $M = 4.06$ ;  $R = 2.7 \times 10^6$ .



(b) Body.

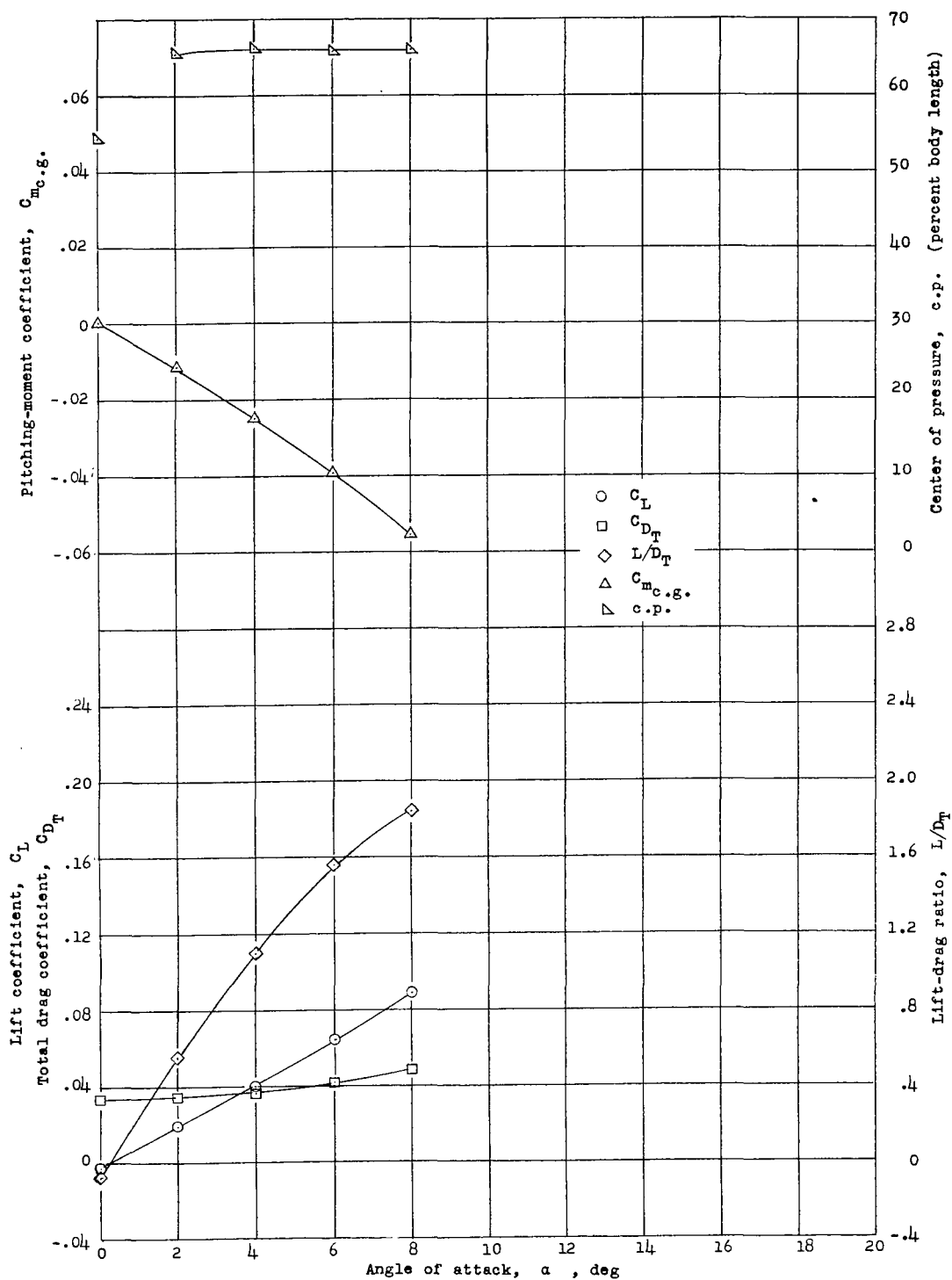
Figure 5.- Continued.



(c) Body-wing.

Figure 5.- Continued.





(d) Body-tail.

Figure 5.- Concluded.

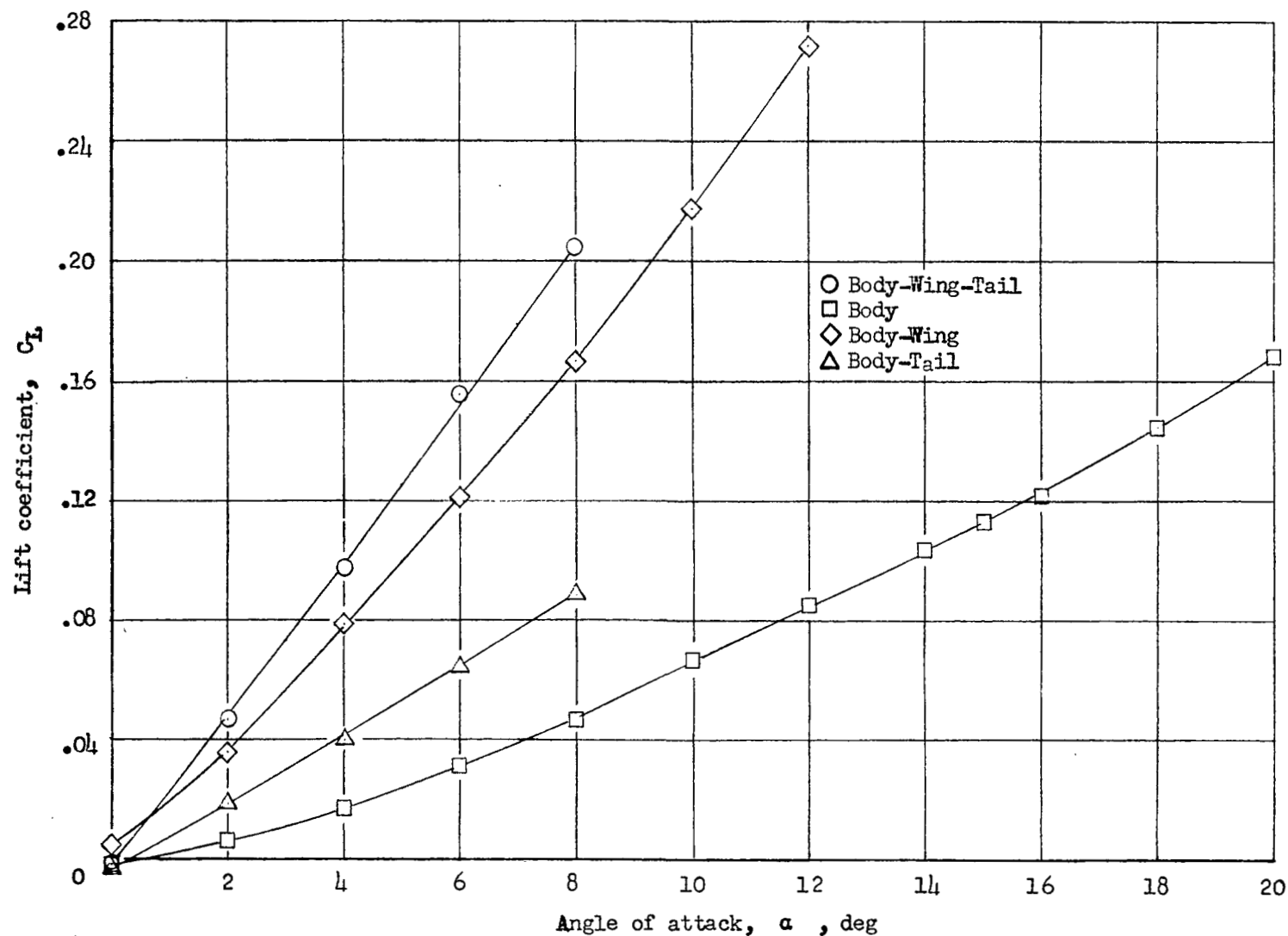


Figure 6.- Variation of lift coefficient with angle of attack for an airplane configuration and its components.  $M = 4.06$ ;  $R = 2.7 \times 10^6$ .

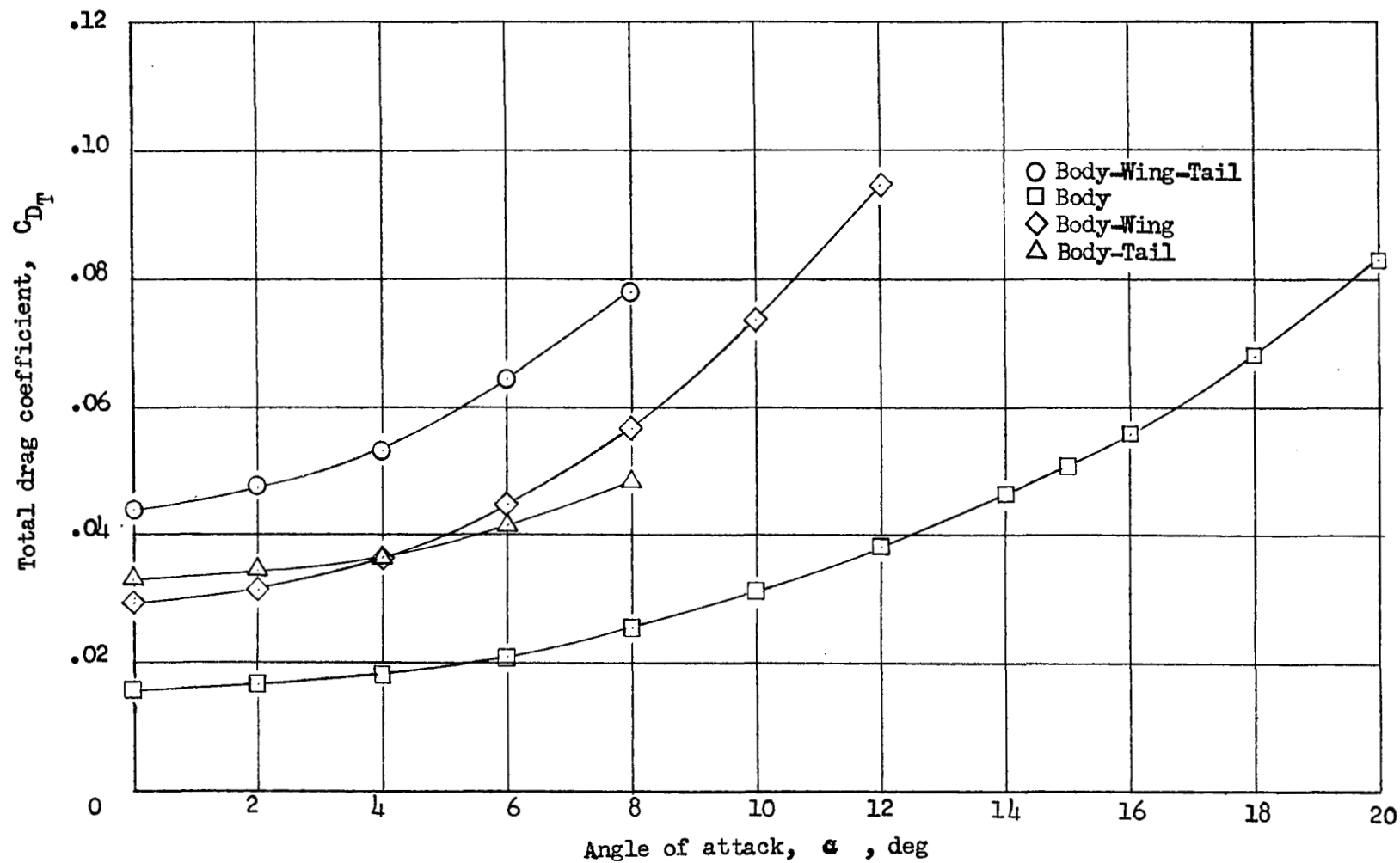


Figure 7.- Variation of total drag coefficient with angle of attack for an airplane configuration and its components.  $M = 4.06$ ;  $R = 2.7 \times 10^6$ .

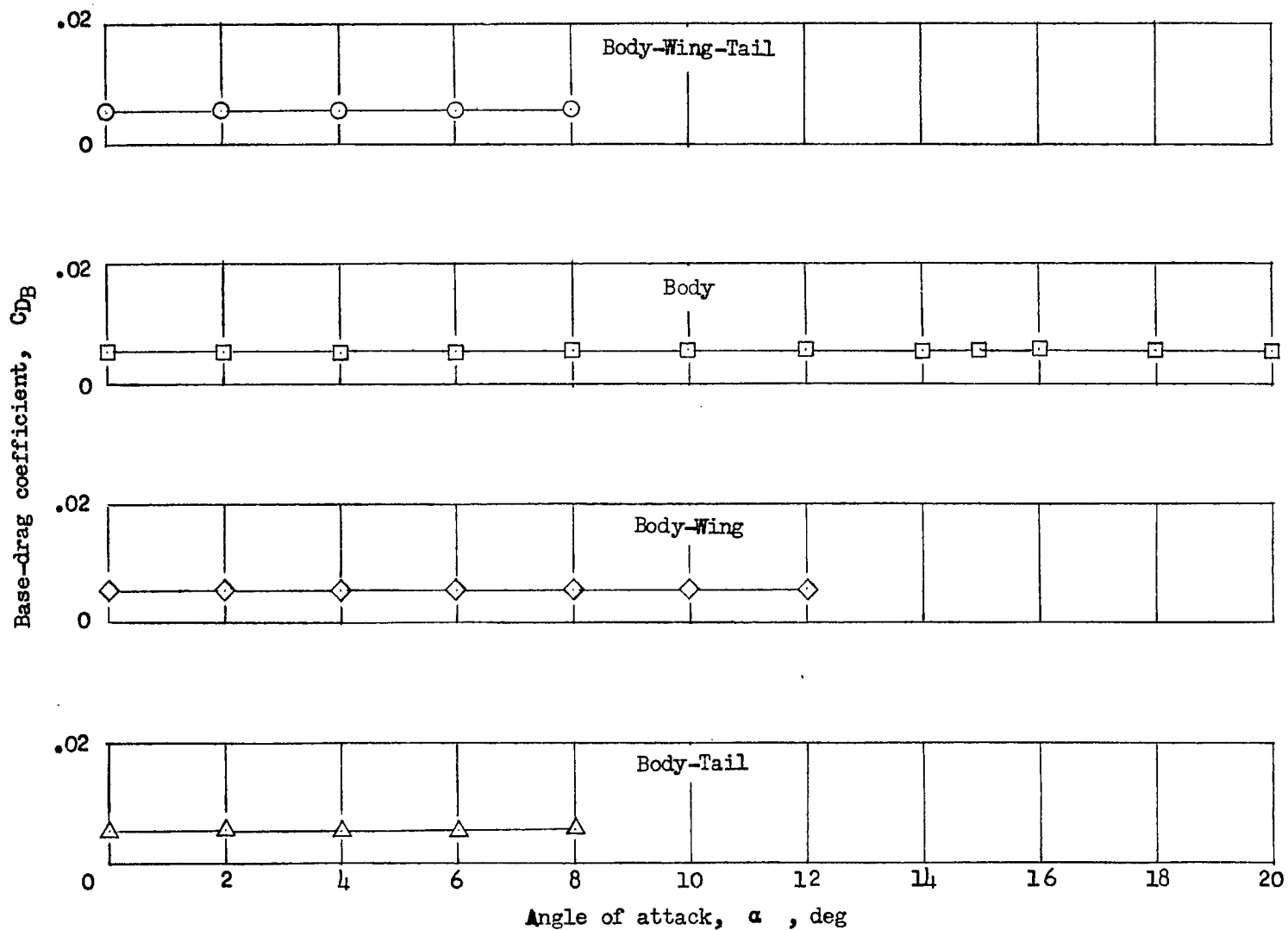


Figure 8.- Variation of base drag coefficient with angle of attack for an airplane configuration and its components.  $M = 4.06$ ;  $R = 2.7 \times 10^6$ .

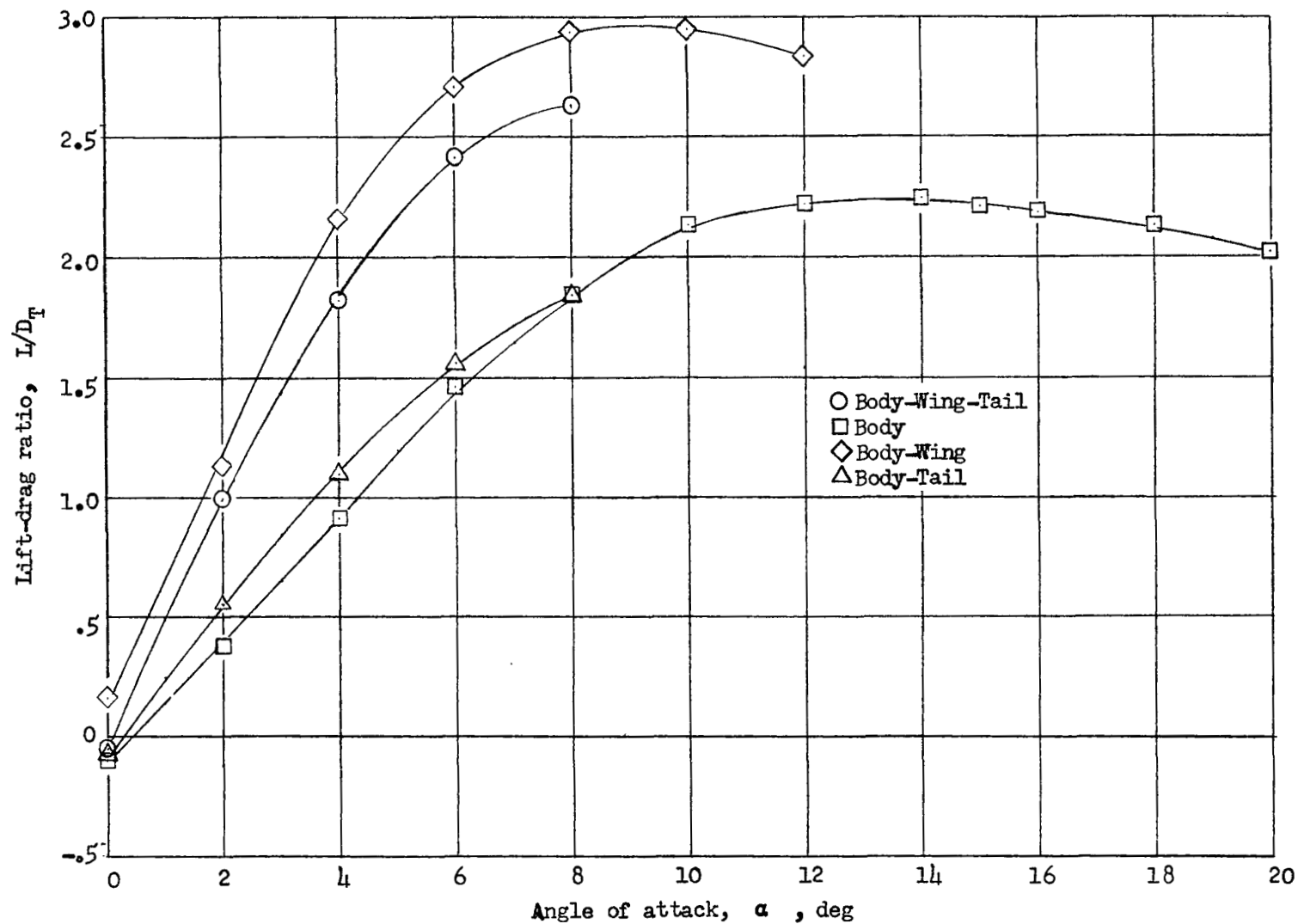


Figure 9.- Variation of lift-drag ratio with angle of attack for an airplane configuration and its components.  $M = 4.06$ ;  $R = 2.7 \times 10^6$ .

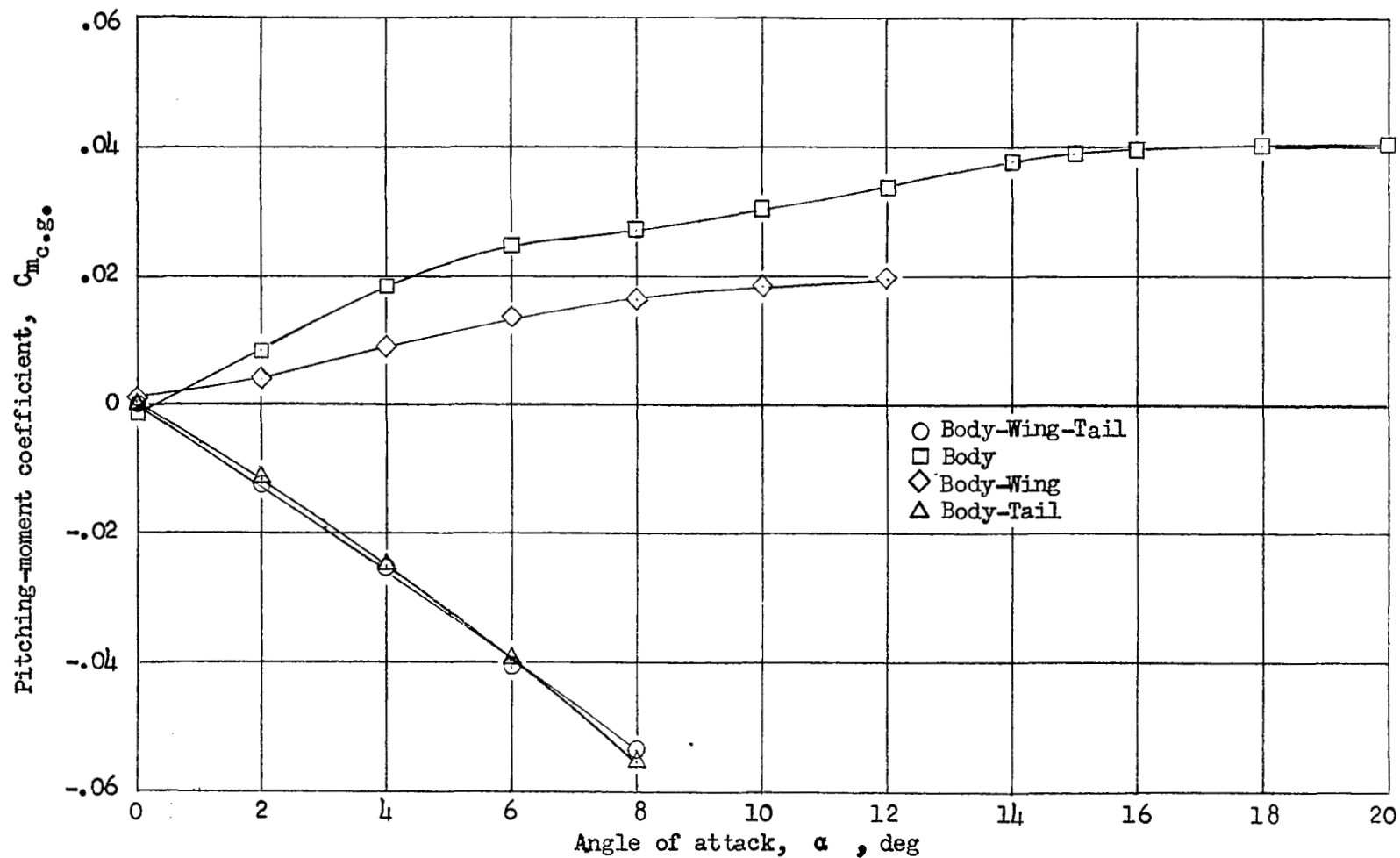


Figure 10.- Variation of pitching-moment coefficient with angle of attack for an airplane configuration and its components.  $M = 4.06$ ;  $R = 2.7 \times 10^6$ .

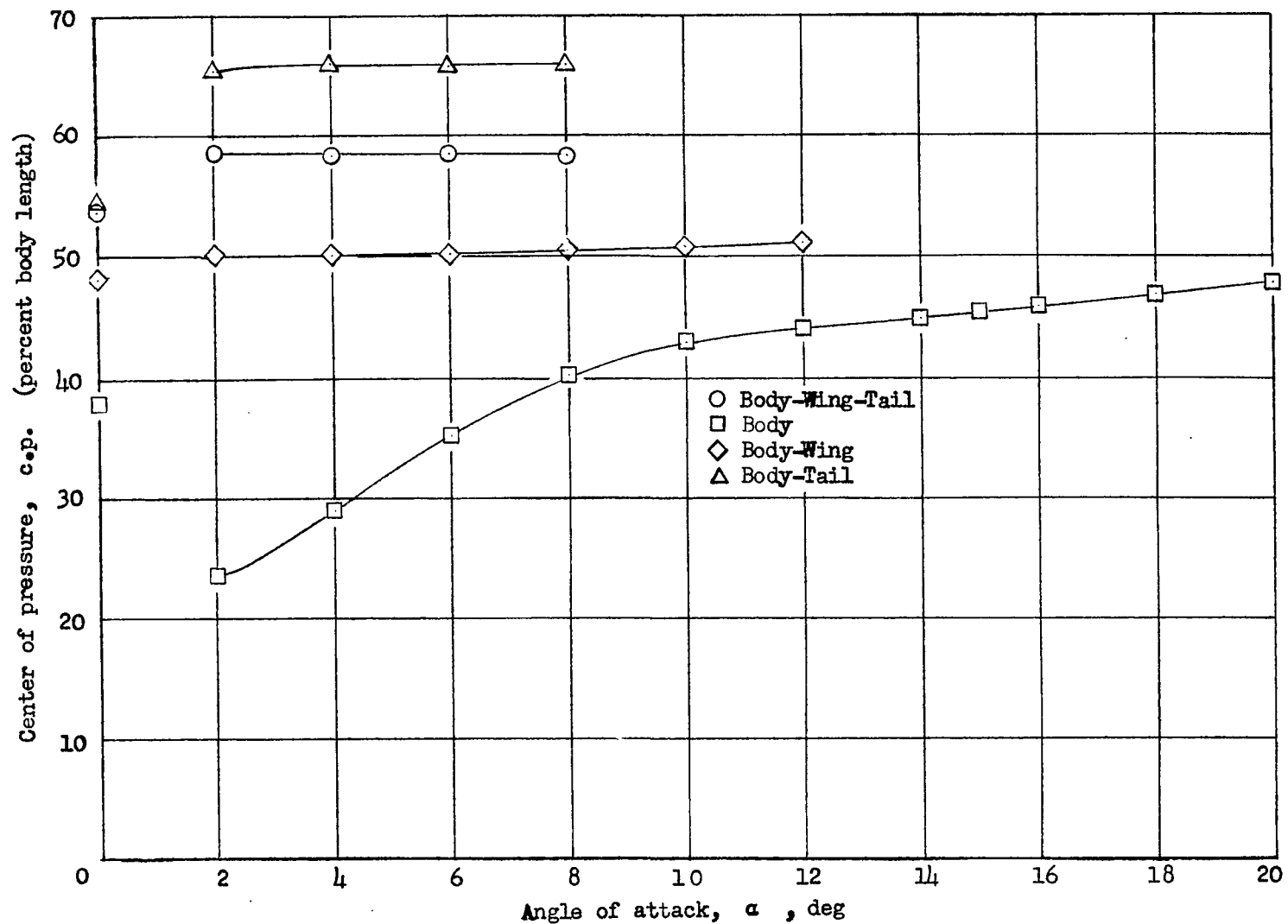


Figure 11.- Variation of longitudinal center of pressure with angle of attack for an airplane configuration and its components.  $M = 4.06$ .

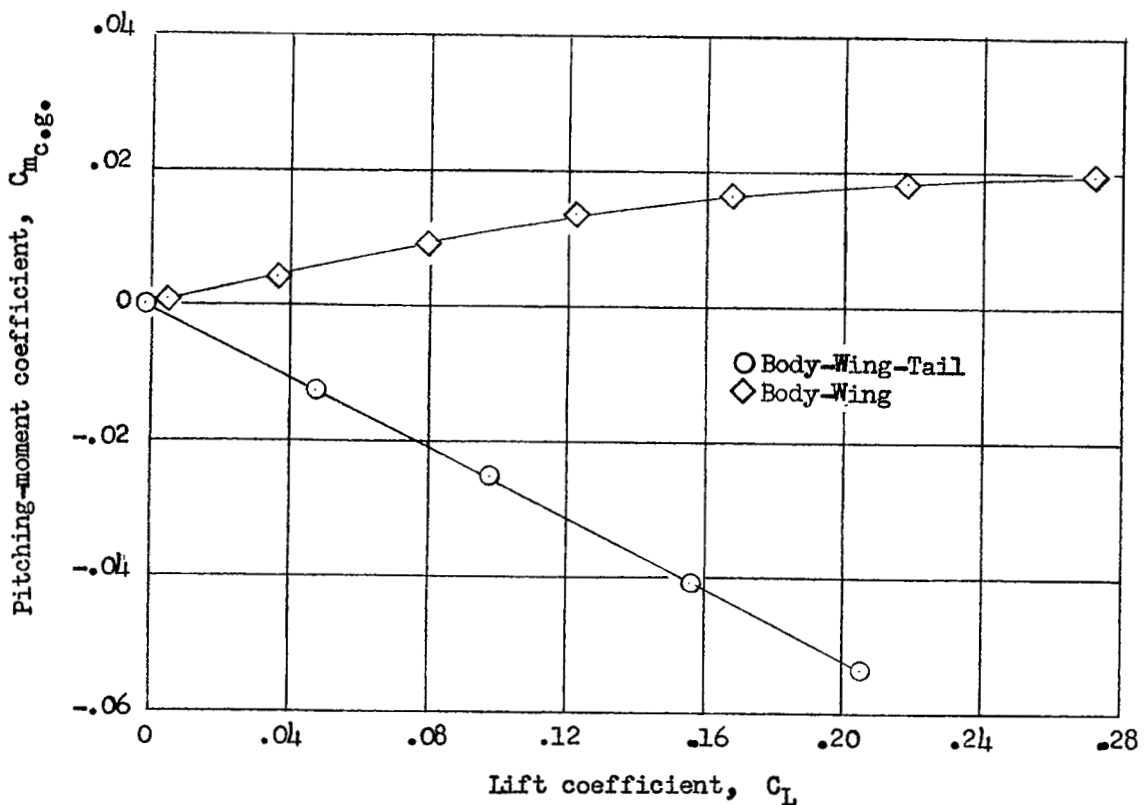


Figure 12.- Variation of pitching-moment coefficient with lift coefficient for an airplane configuration with and without tail fins.  $M = 4.06$ .

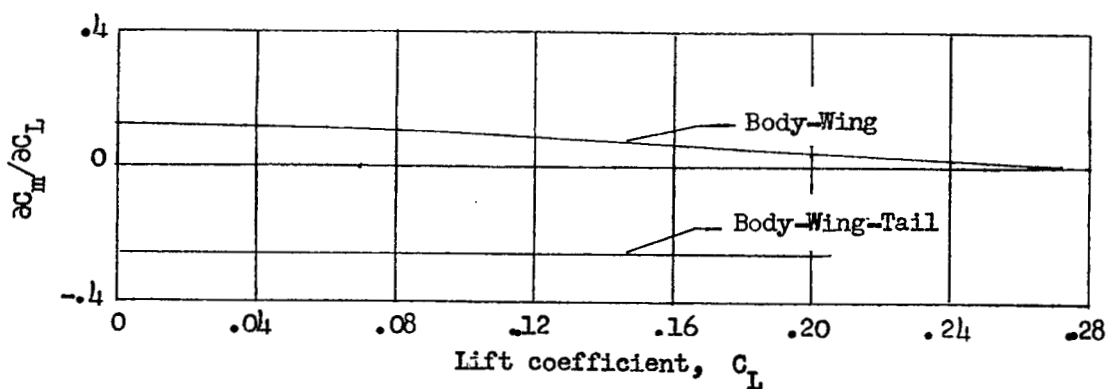


Figure 13.- Variation of the static-longitudinal-stability parameter  $\frac{\partial C_m}{\partial C_L}$  with lift coefficient for the complete model and for the body-wing configuration.  $M = 4.06$ .



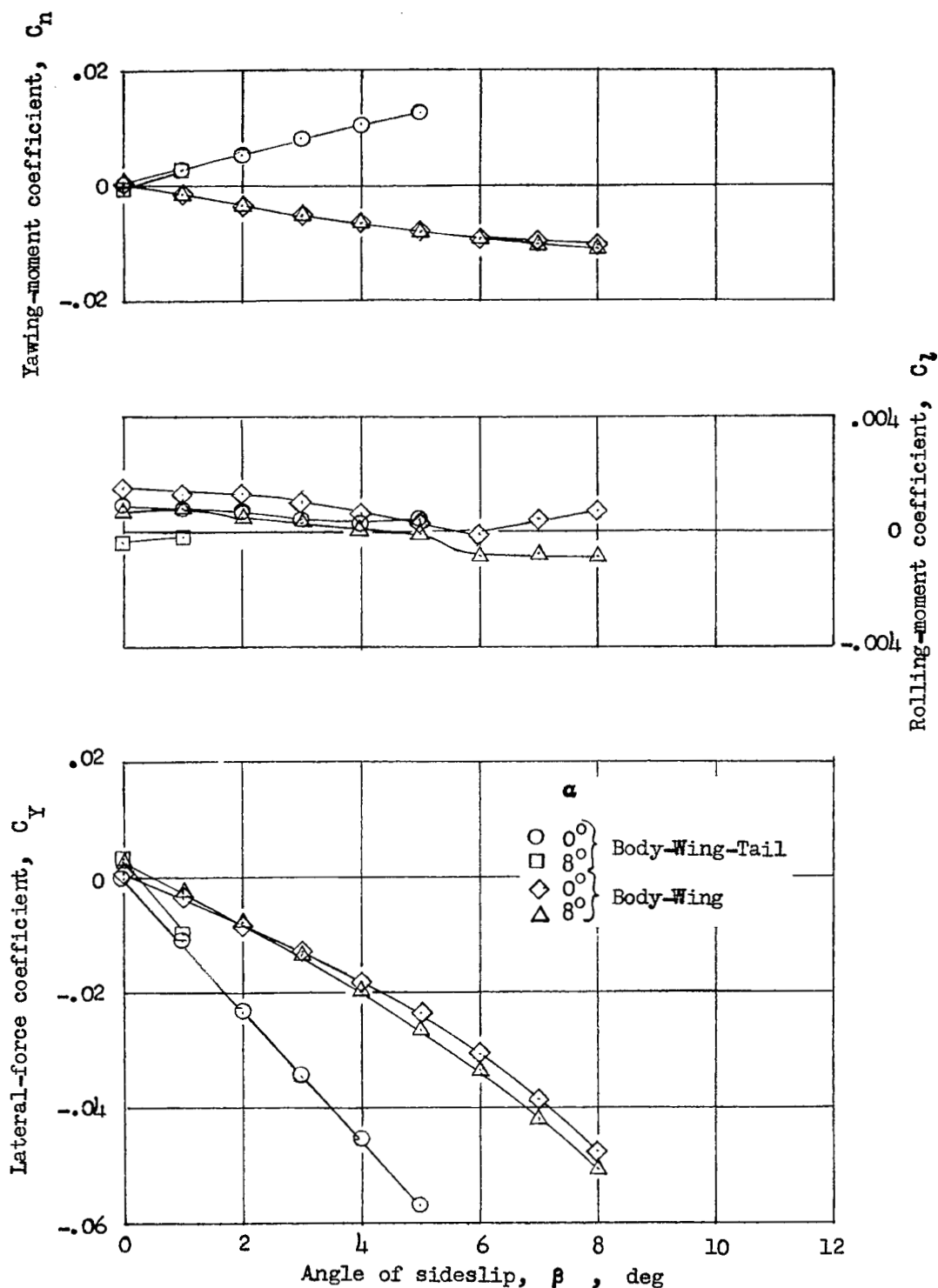


Figure 14.- Variation with angle of sideslip of the static lateral characteristics for an airplane configuration with and without tail fins.  $M = 4.06$ ;  $R = 2.7 \times 10^6$ .

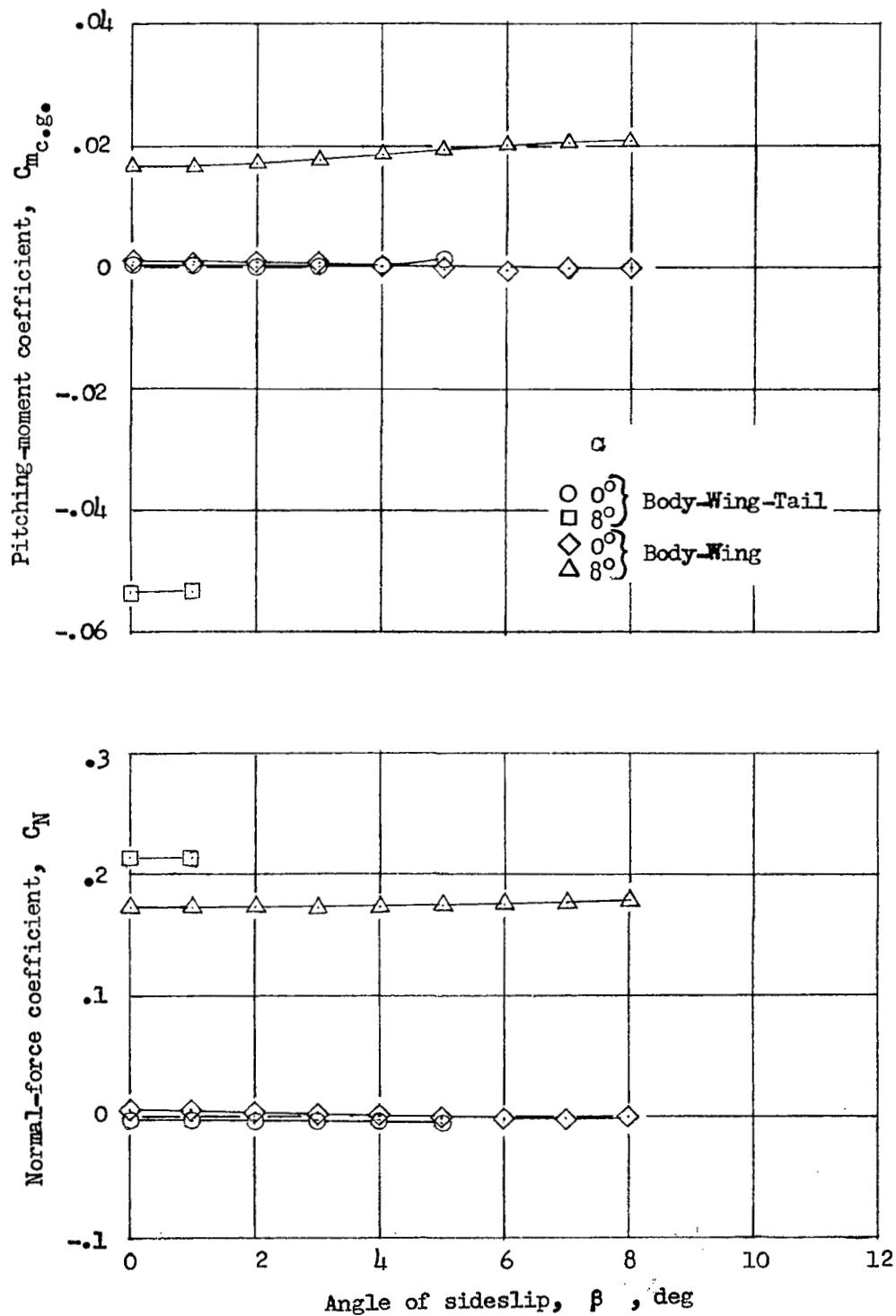


Figure 15.- Variation with angle of sideslip of the static longitudinal characteristics for an airplane configuration with and without tail fins.  $M = 4.06$ ;  $R = 2.7 \times 10^6$ .

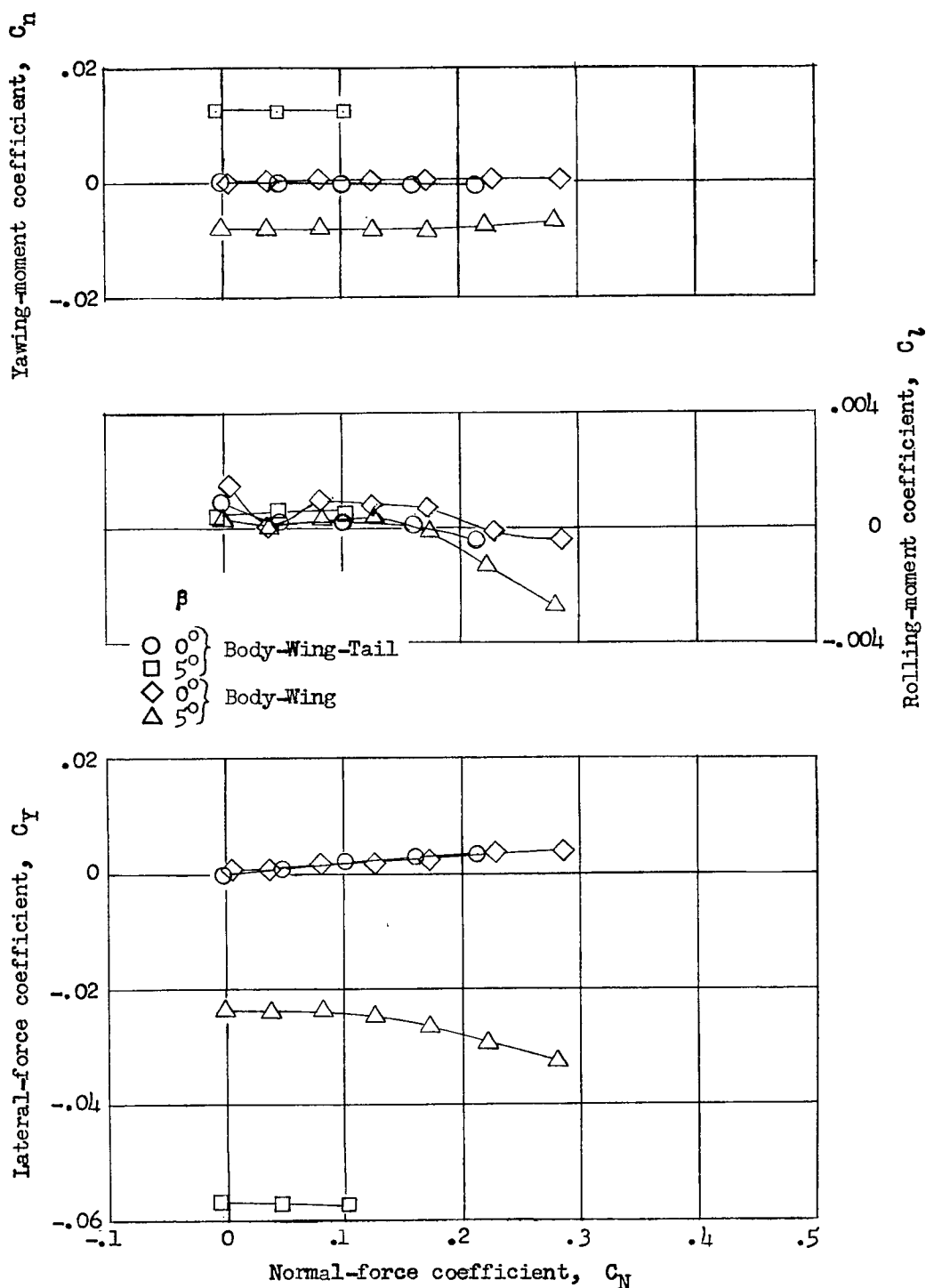


Figure 16.- Variation with normal-force coefficient of the static lateral characteristics for an airplane configuration with and without tail fins.  $M = 4.06$ ;  $R = 2.7 \times 10^6$ .

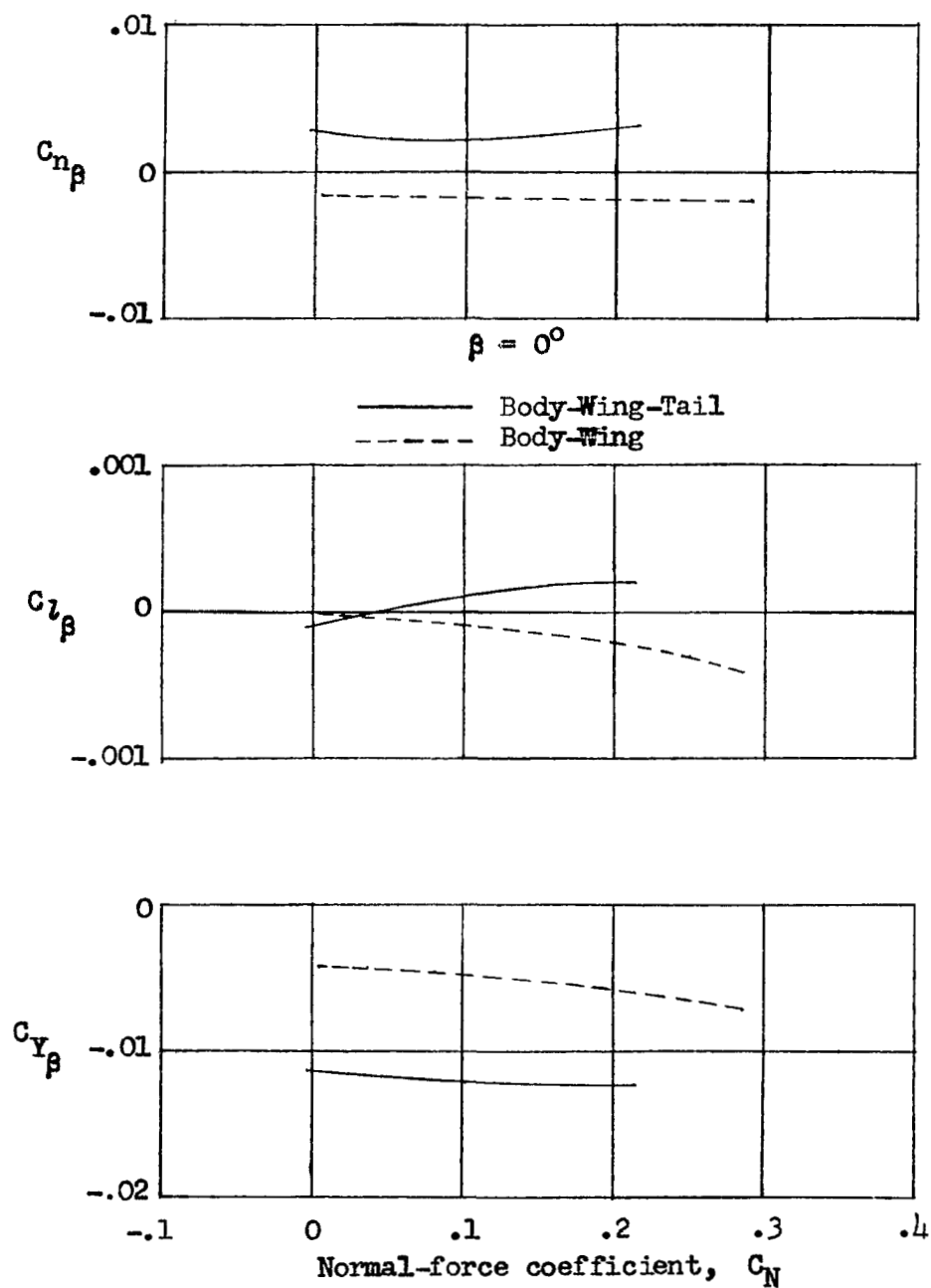
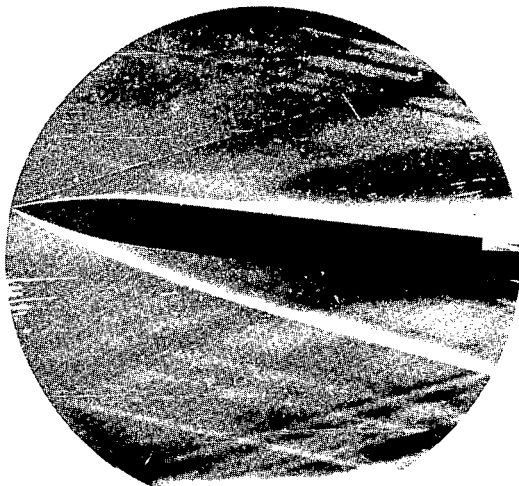


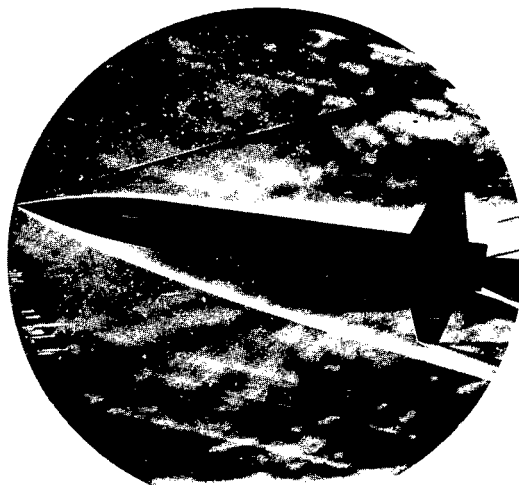
Figure 17.- Variation with normal-force coefficient of the rate of change of the static lateral force coefficients with  $\beta$  for an airplane configuration with and without tail fins.  $M = 4.06; R = 2.7 \times 10^6$ .



Body alone



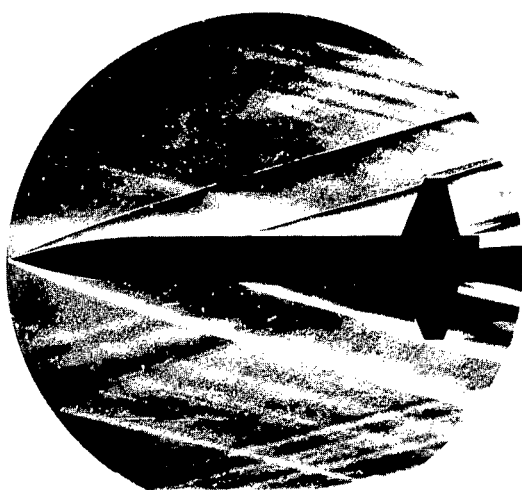
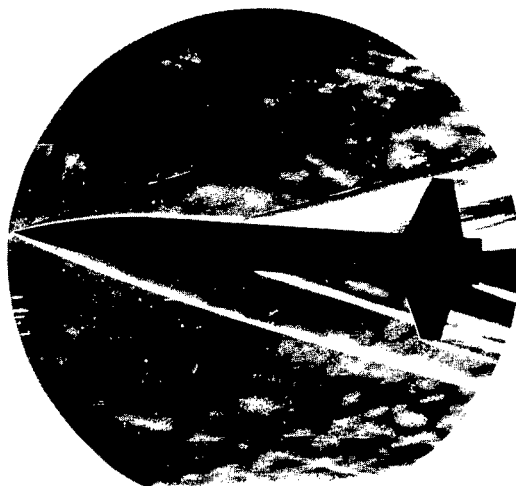
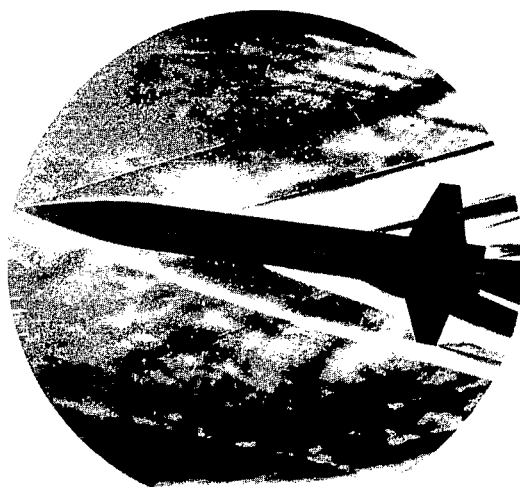
Body-wing



Body-tail

L-87529

Figure 18.- Schlieren photographs of the flow around the body-alone, body-wing, and body-tail configurations.  $\alpha = 8^\circ$ ;  $\beta = 0^\circ$ ;  $M = 4.06$ .

 $\alpha = 0^\circ$  $\alpha = 4^\circ$  $\alpha = 8^\circ$ 

L-87530

Figure 19.- Schlieren photographs of the flow around the complete-airplane configuration.  $\beta = 0^\circ$ ;  $M = 4.06$ .